Lecture # 30: Incompressible Flow over an Airfoil – Part 06 : Separation Bubbles

Dr. Hui HU
Department of Aerospace Engineering
Iowa State University, 2251 Howe Hall, Ames, IA 50011-2271
Tel: 515-294-0094 / Email: huhui@iastate.edu

❑ Thin Airfoil Theory

Principle:

- ***Replace thin airfoil with the mean camber line (MCL) because of the small thickness and camber of the airfoil***
- ***MCL assumed to be a streamline of the flow around the thin airfoil.***
- ***To force the MCL to be a streamline, the sum of all velocity components normal to the MCL must be equal to zero.***

$$V_{\infty,n} + V_{vortex-induced,n} = 0$$

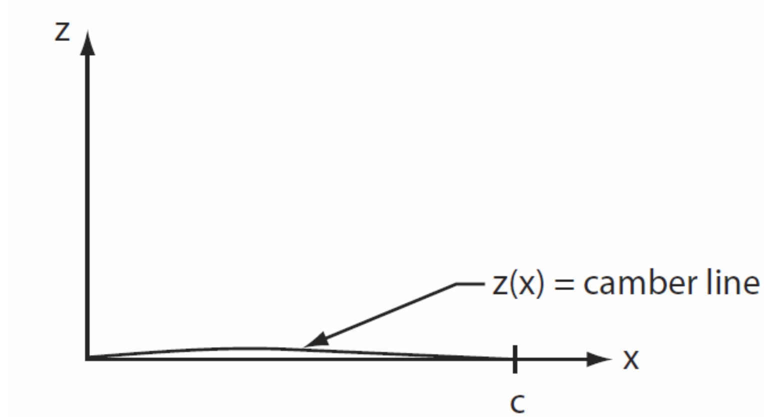

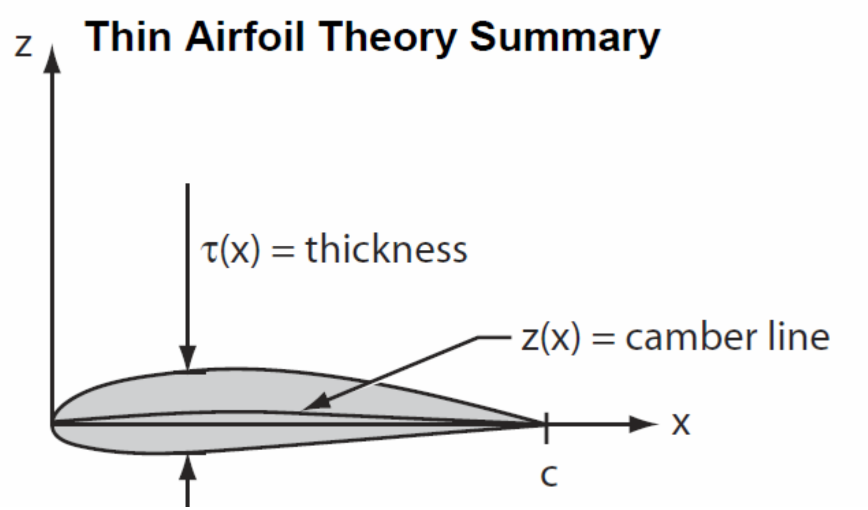

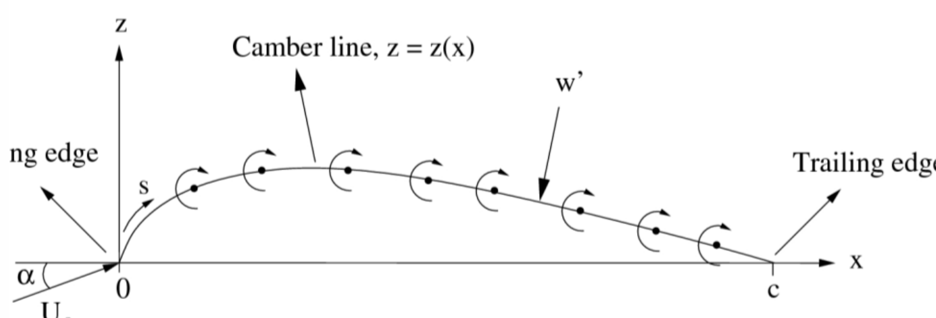

(b) Vorticity distribution on the camber line of the airfoil

❑ Thin Airfoil Theory – Cambered Airfoil

❑ *Lift coefficient of a cambered airfoil*

$$L = \rho V_\infty \Gamma = \rho V_\infty{}^2 c[A_0\pi + \frac{\pi}{2}A_1]$$

$$C_L = \frac{L}{\frac{1}{2}\rho V_\infty{}^2 c} = \frac{\rho V_\infty{}^2 c[A_0\pi + \frac{\pi}{2}A_1]}{\frac{1}{2}\rho V_\infty{}^2 c} = 2\pi[A_0 + A_1/2]$$

$$\because A_0 = \alpha + B_0 = \alpha - \frac{1}{\pi}\int_0^\pi \frac{dz}{dx}d\theta; \quad A_1 = \frac{2}{\pi}\int_0^\pi \frac{dz}{dx}\cos(\theta)d\theta$$

$$\therefore C_L = 2\pi[\alpha - \frac{1}{\pi}\int_0^\pi \frac{dz}{dx}(1-\cos\theta)d\theta]$$

$$\alpha_{L0} = \frac{1}{\pi}\int_0^\pi \frac{dz}{dx}(1-\cos\theta)d\theta$$

$$C_L = 2\pi[\alpha - \alpha_{L0}]$$

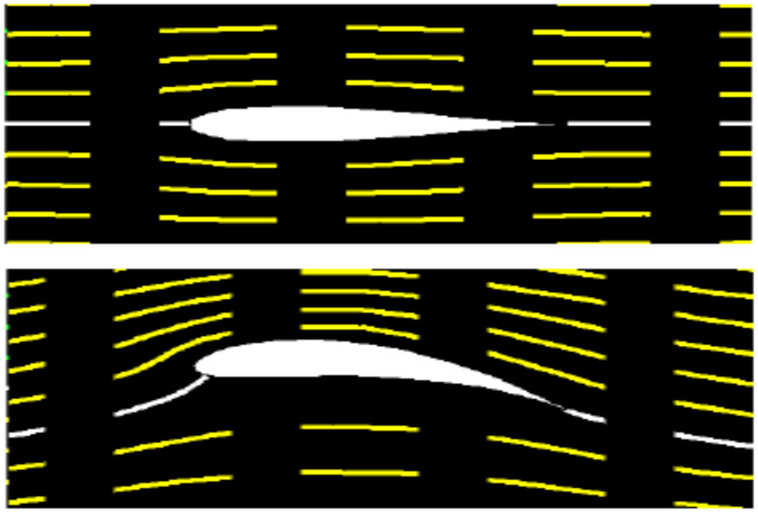

- ***The value of α_{L0} will be determined if the MCL is given for an airfoil, which is not a function of α.***
- ***The slope of the Lift coefficient profile is still 2π.***

$$\frac{dC_L}{d\alpha} = 2\pi$$

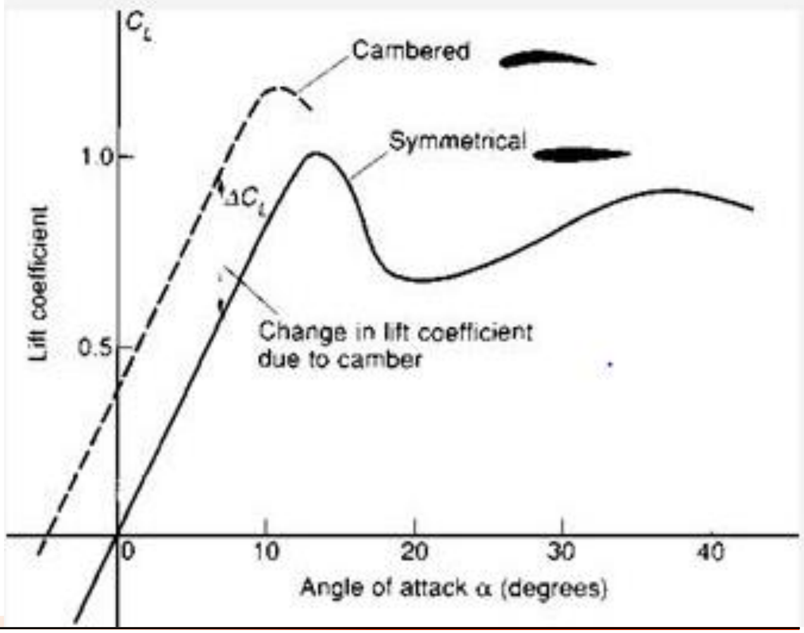

❑ Thin Airfoil Theory – Cambered Airfoil

❑ *Moment about the airfoil leading edge*

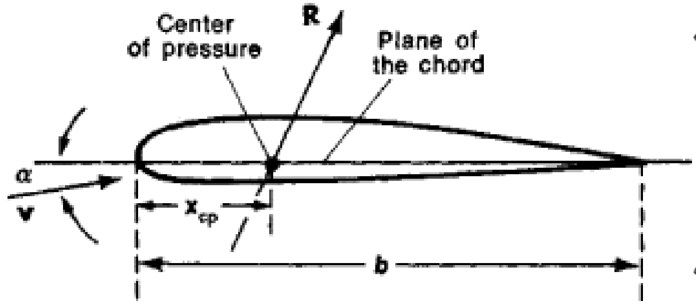

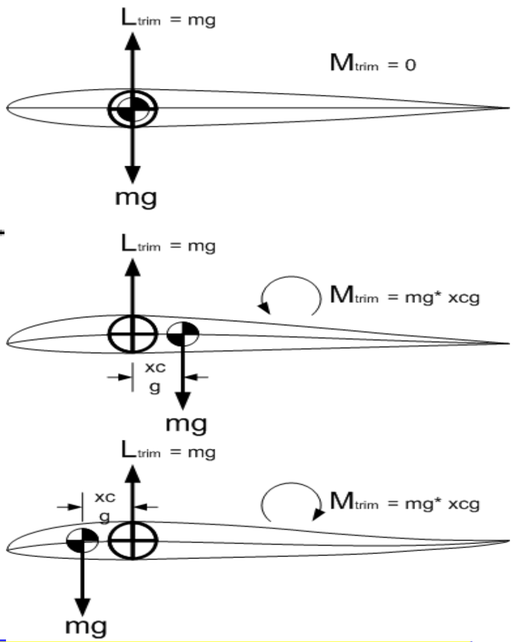

$$M_{LE} = -\int_{LE}^{TE} x dL; \quad dL = \rho V_\infty \gamma(x) dx$$

$$\Rightarrow M_{LE} = -\int_{LE}^{TE} x \cdot \rho V_\infty \gamma(x) dx$$

$$\because x = \frac{c}{2}(1-\cos\theta); \quad \gamma(\theta) = 2\alpha V_\infty \frac{1+\cos\theta}{\sin\theta}$$

$$\therefore dx = \frac{c}{2}\sin\theta d\theta$$

$$\Rightarrow M_{LE} = -\int_{LE}^{TE} x \rho V_\infty \gamma(x) dx$$

$$= -\int_{LE}^{TE} \frac{c}{2}(1-\cos\theta)\cdot \rho V_\infty \cdot 2V_\infty [A_0 \frac{1+\cos\theta}{\sin\theta} + \sum_{n=1}^{\infty} A_n \sin(n\theta)] \cdot \frac{c}{2}\sin\theta d\theta$$

Therefore:

$$C_{M,LE} = \frac{M_{LE}}{\frac{1}{2}\rho V_\infty{}^2 c^2} = -A_0\frac{\pi}{2} - A_1\frac{\pi}{2} + A_2\frac{\pi}{4}$$

$$A_n = \frac{2}{\pi}\int_0^\pi \frac{dz}{dx}\cos(n\theta)d\theta$$

Therefore:

$$\because C_L = 2\pi A_0 + A_1\pi;$$

$$\therefore C_{M,LE} = -\frac{\pi}{2}[\frac{2A_0 + A_1 - A_2}{2}] = -[\frac{C_L}{4} + \frac{\pi}{4}(A_1 - A_2)]$$

$$\because C_{M,LE} = C_{M,c/4} - \frac{C_L}{4}$$

$$\therefore C_{M,c/4} = -\frac{\pi}{4}(A_1 - A_2)$$

$$x_{CP} = \frac{1}{4}(c + \frac{\pi c}{C_L}(A_1 - A_2))$$

- ***No dependency on α for aerodynamic center***

Thin Airfoil Theory – Cambered Airfoil

- *Center of Lift or center of pressure on an airfoil*

$$c_l = 2\pi\alpha$$

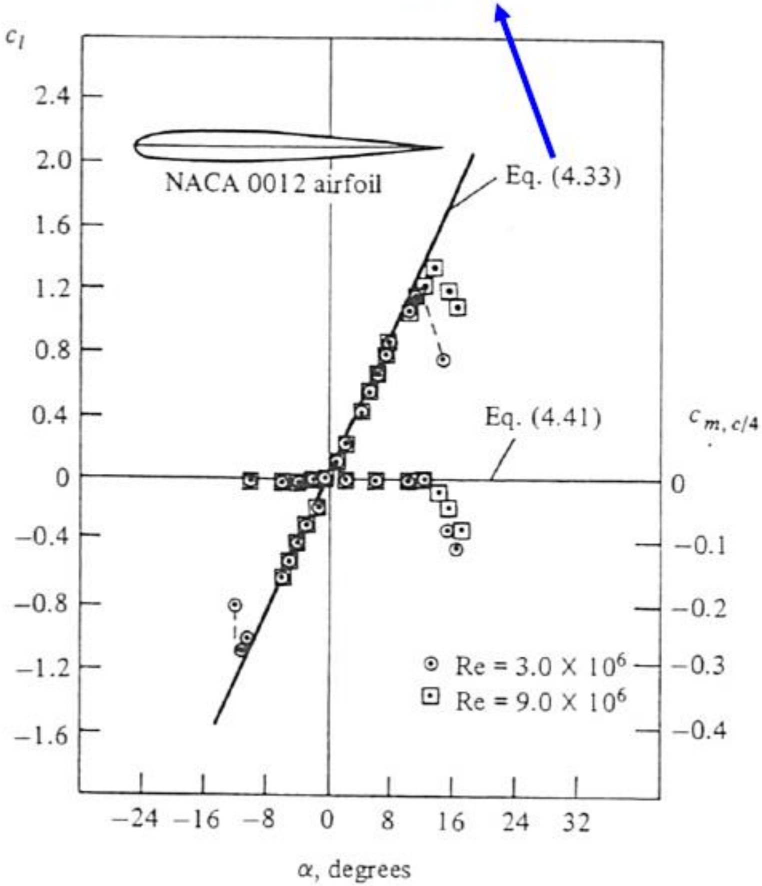

$$C_{M,c/4} = 0$$

$$c_l = 2\pi(\alpha - \alpha_{L=0})$$

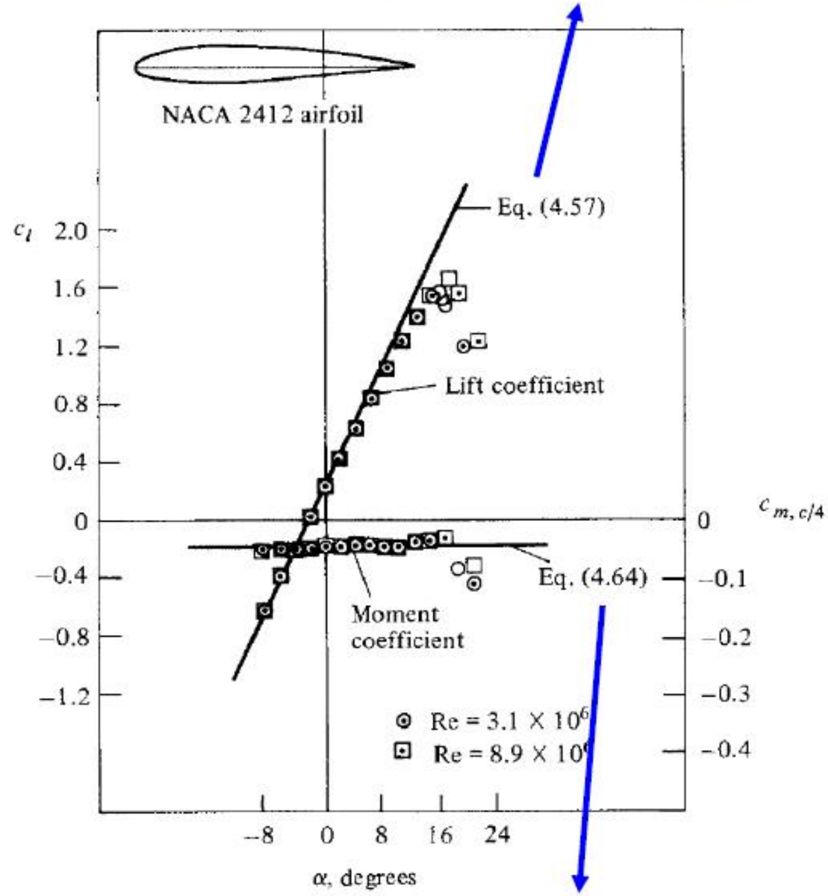

$$C_{M,c/4} = -\frac{\pi}{4}(A_1 - A_2)$$

❑ Thin Airfoil Theory

Assumptions:

- ***2-dimensions***
- ***Potential flows***
- ***Small α***
- ***Small max τ /c (i.e., airfoil thickness)***
- ***Small max z/ c ((i.e., airfoil camber)***

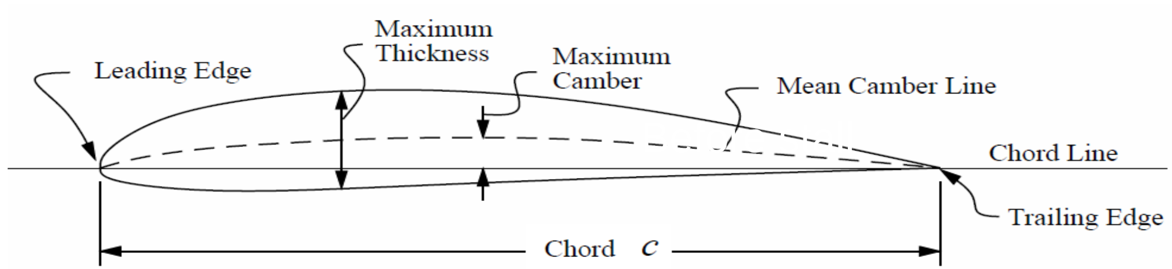

$$C_l = \frac{L}{\frac{1}{2}\rho V_\infty^2 c}$$

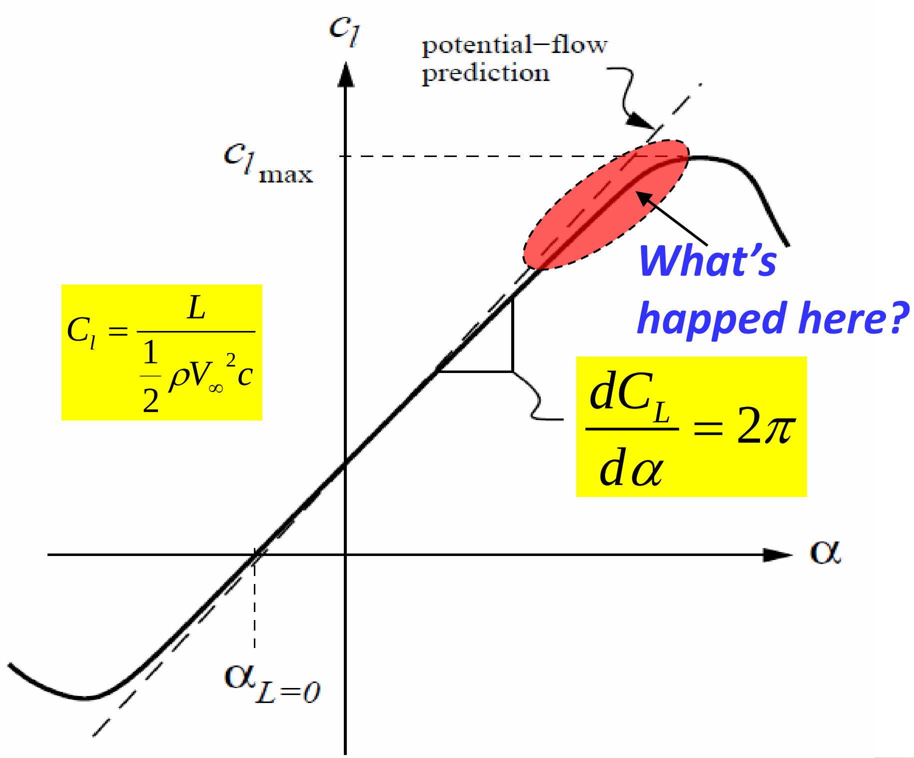

$$\frac{dC_L}{d\alpha} = 2\pi$$

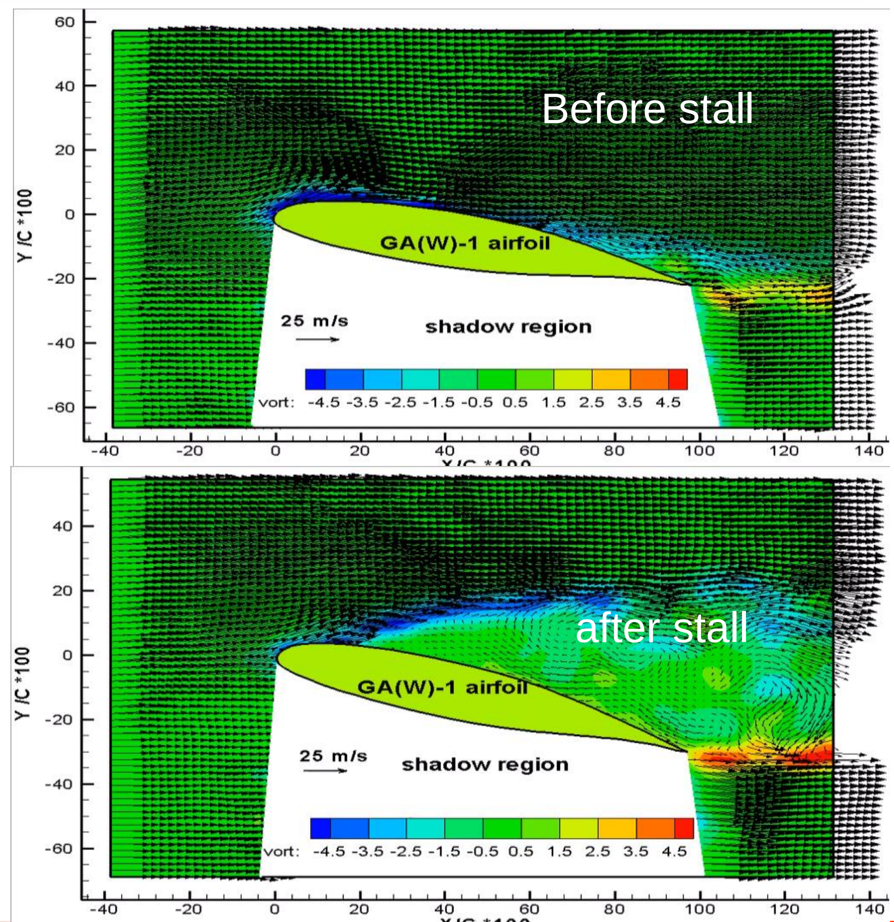

Flow Separation and Transition on Low-Reynolds-number Airfoils

- *Since laminar boundary layers are unable to withstand any significant adverse pressure gradient, laminar flow separation is usually found on low-Reynolds-number airfoils. Post-separation behavior of the laminar boundary layers would affect the aerodynamic performances of the low-Reynolds-number airfoils ($Re<10^6$) significantly.*
- *Separation bubbles are usually found to form on the upper surfaces of low-Reynolds-number airfoils . Separation bubble would burst suddenly to cause airfoil stall at high AOA when the adverse pressure gradient becoming too big.*

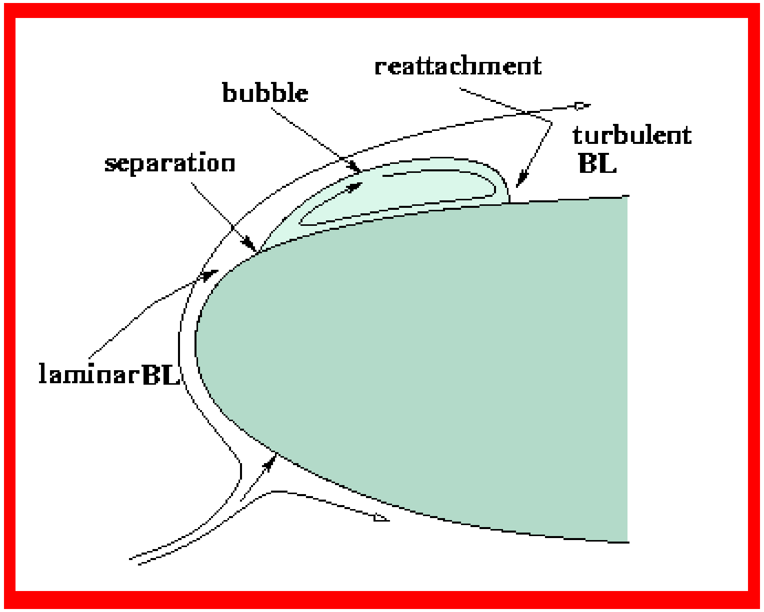

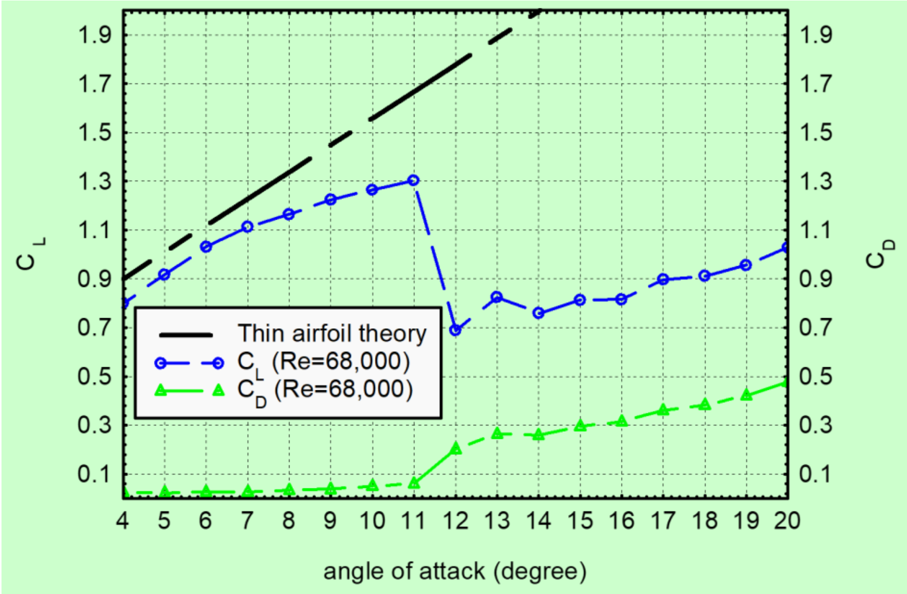

The GA(W)-1 Airfoil Used in the Present Study

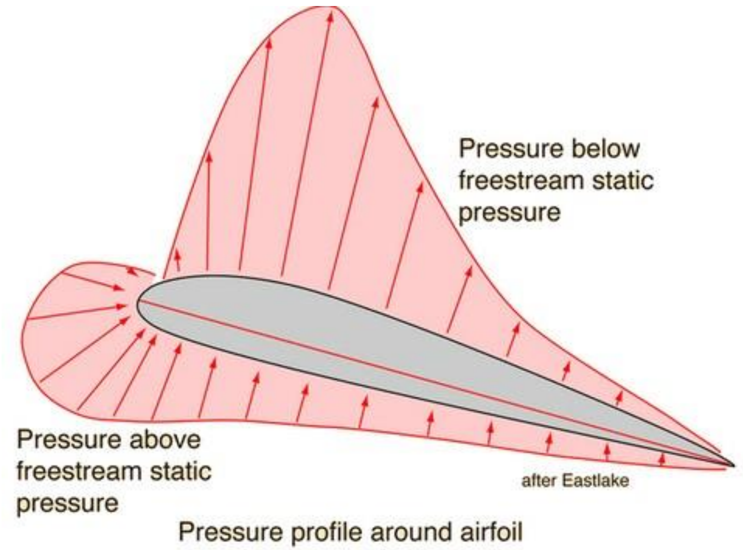

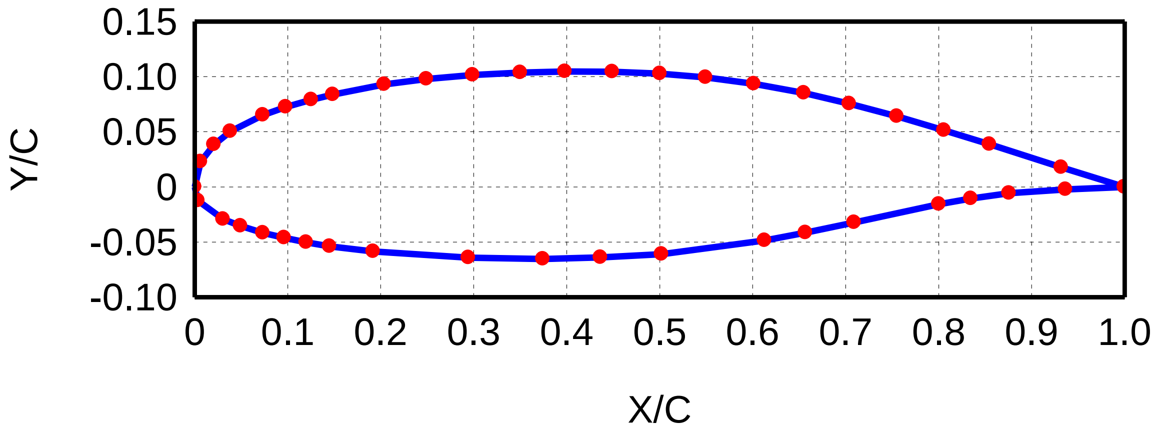

- ***The GA(W)-1 Airfoil***

DSA3217 (Shown)

Surface Pressure Coefficient distributions (Re=68,000)

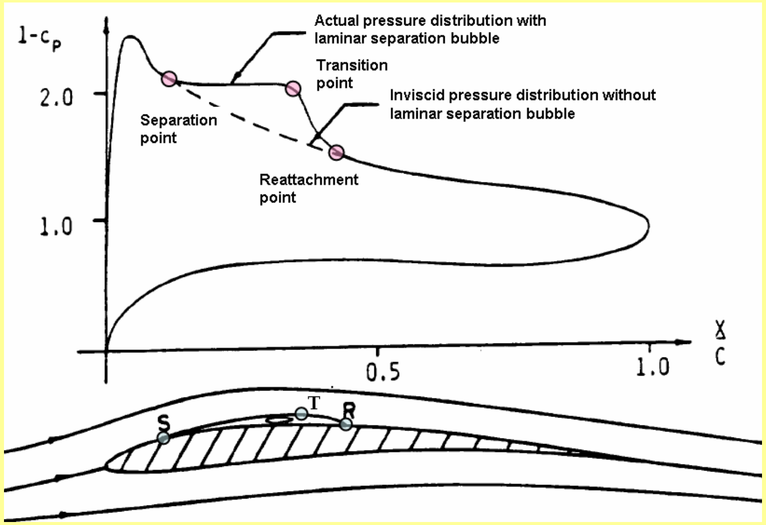

Typical surface pressure distribution when a laminar separation bubble is formed (Russell, 1979)

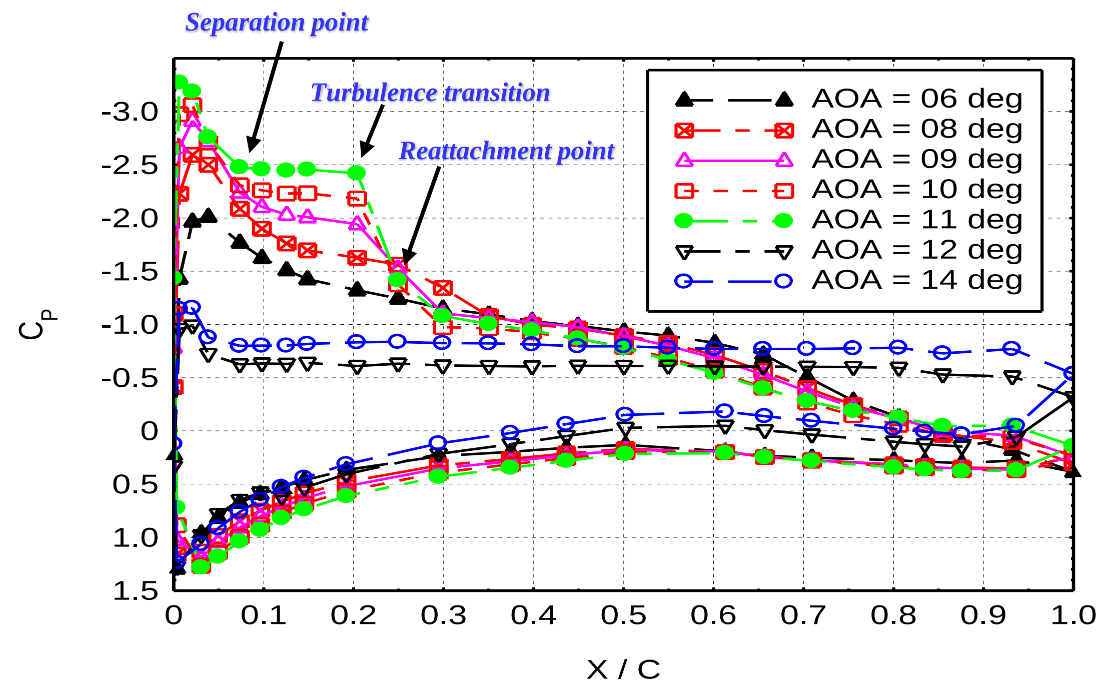

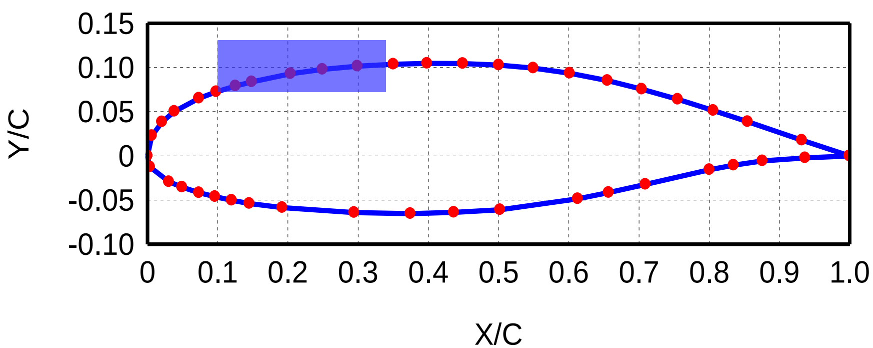

GA (W)-1 airfoil

(also labeled as NASA LS(1)-0417)

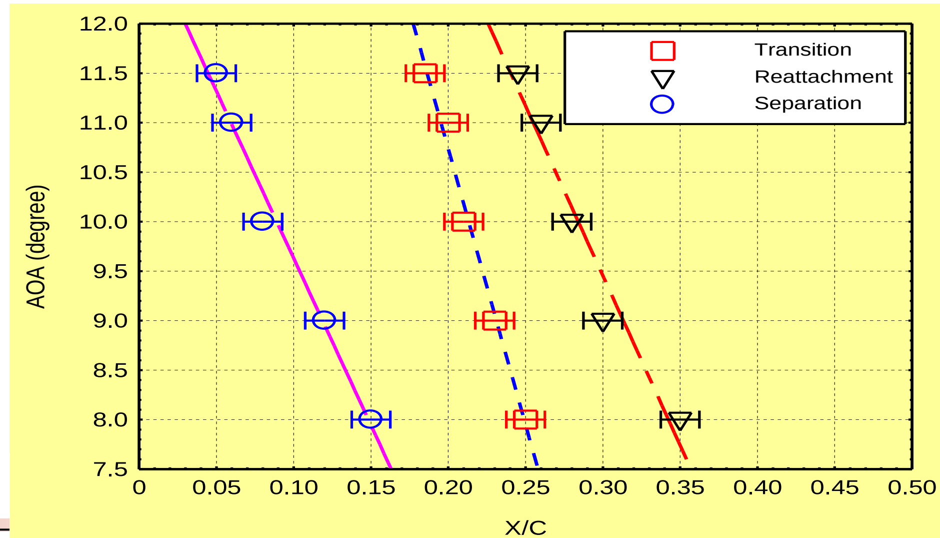

IOWA *(Hu et al., Journal of Fluid Engineering, 2009)*

Measured lift and drag coefficients

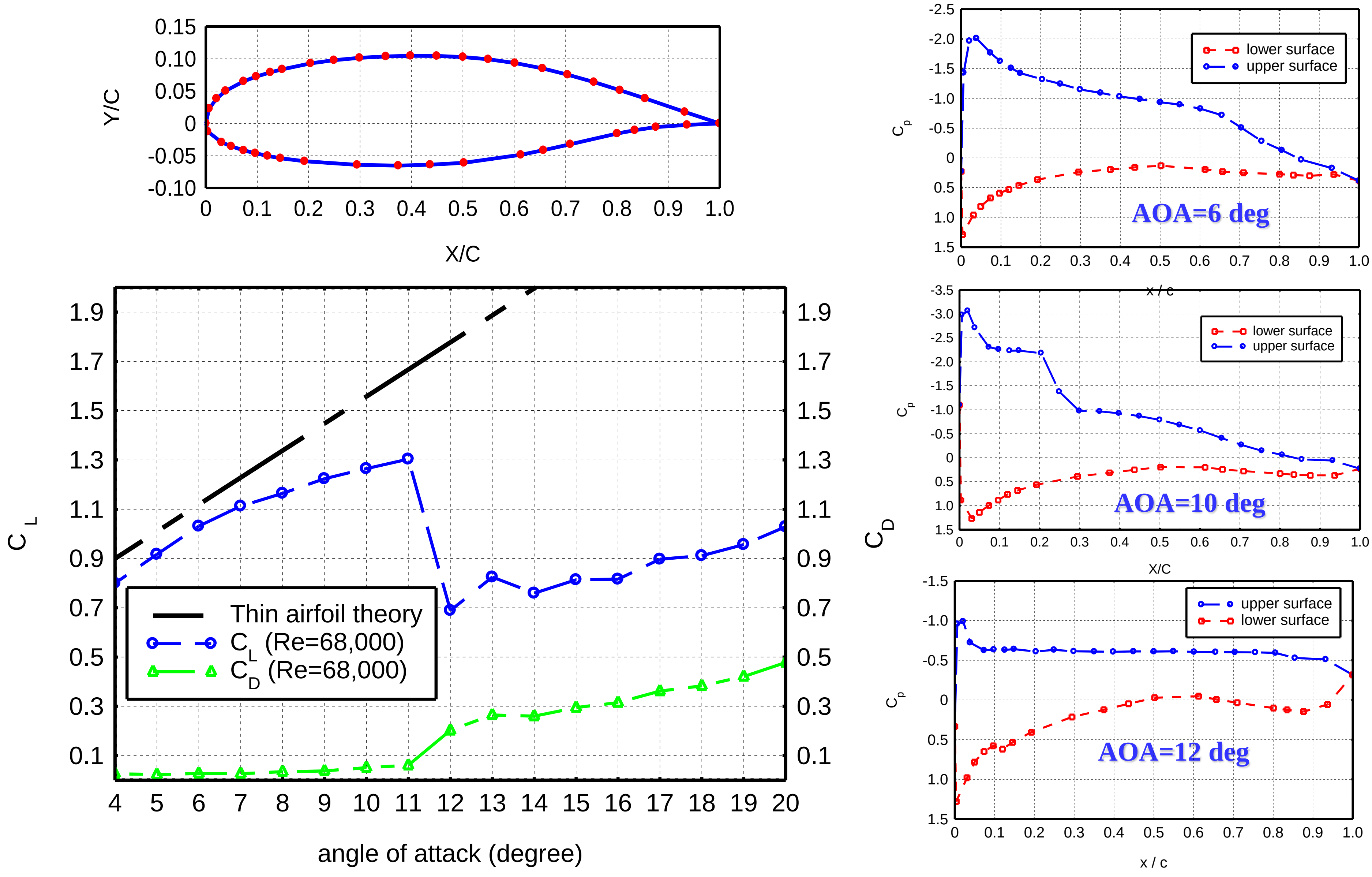

Experimental Setup for PIV Measurements

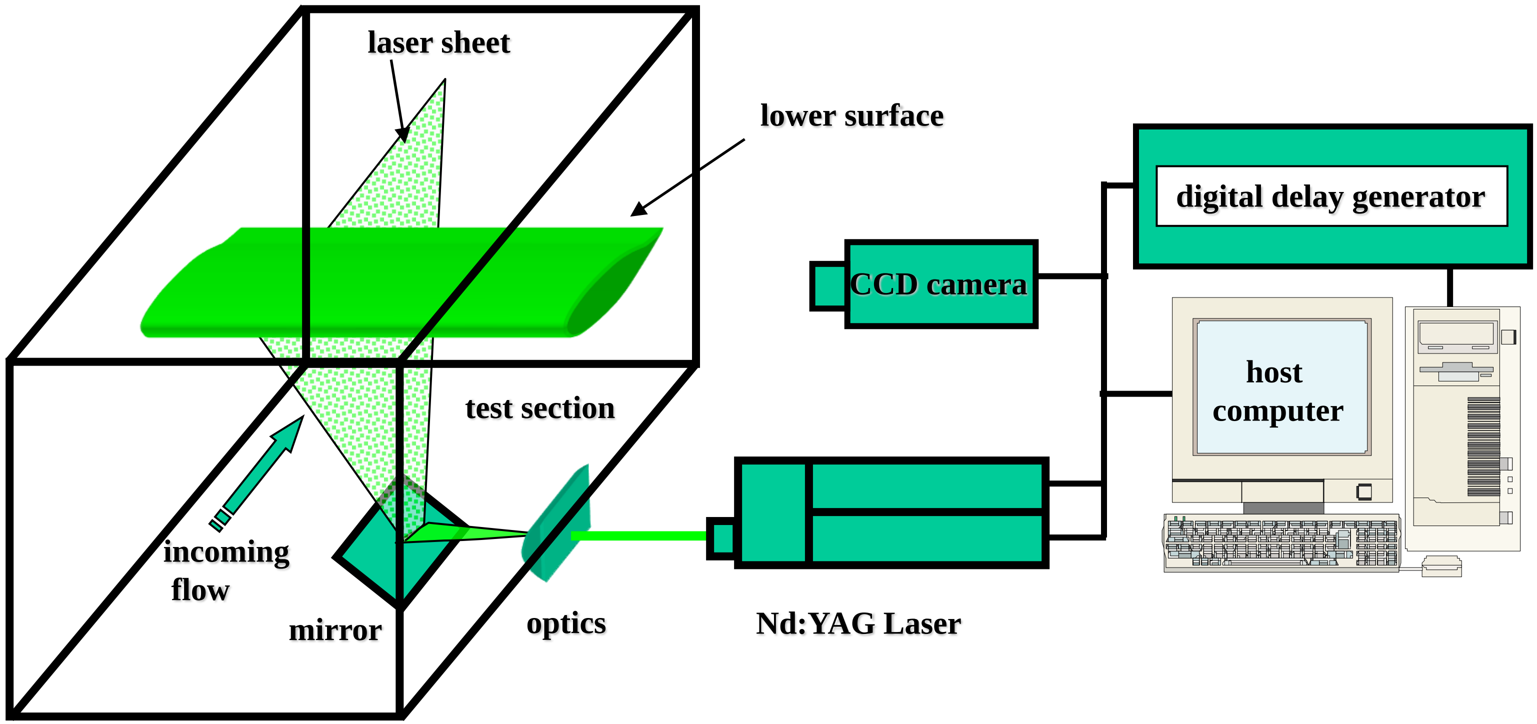

Experimental conditions:

Incoming flow velocity: $U_\infty = 10.0 \; m/s, \quad Re_C = 68{,}000$

Angle of Attack: $20 \geq \alpha \geq 0$

Three Spatial Resolution Levels of the PIV Measurements

Level 1:

- *A coarse level to study the global features of the flow structures around the airfoil.*
- *Measurement window size: 160mm×140mm*
- *Effective resolution: Δ/C = 0.04*

Level 2:

- *A refined level to investigate the detailed features of the laminar boundary layer near the nose of the airfoil.*
- *Measurement window size: 40mm × 30mm*
- *Effective resolution: Δ/C = 0.01*

Level 3:

- *A super-fine level to elucidate the unsteady Kelvin-Helmholtz vortex shedding, the turbulence transition of the shear layer, and the reattachment of the separated boundary layer at the rear end of the separation bubble.*
- *Measurement window size: 14mm × 8mm.*
- *Effective resolution: Δ/C = 0.0035*

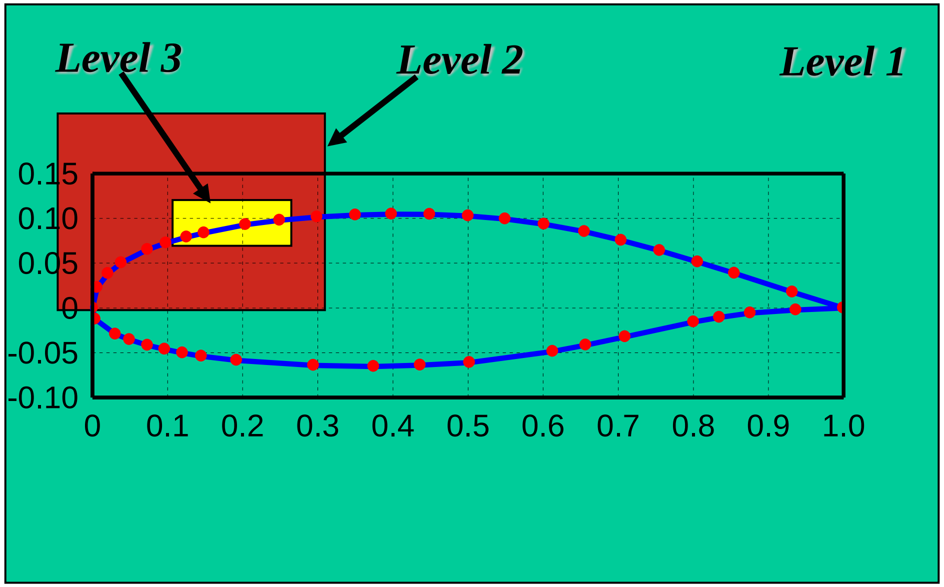

PIV Measurement Results

(AOA=6.0 deg, Re=68,000, spatial resolution $\Delta/C \approx 0.04$)

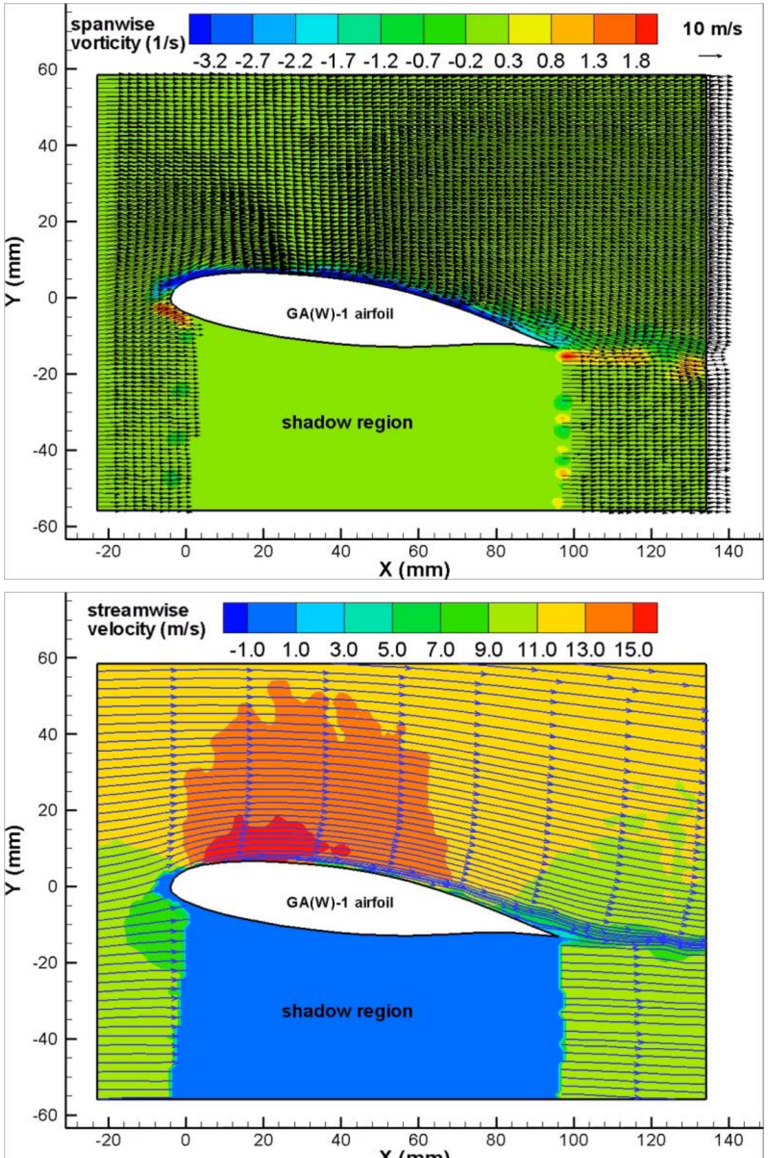

A. instantaneous results

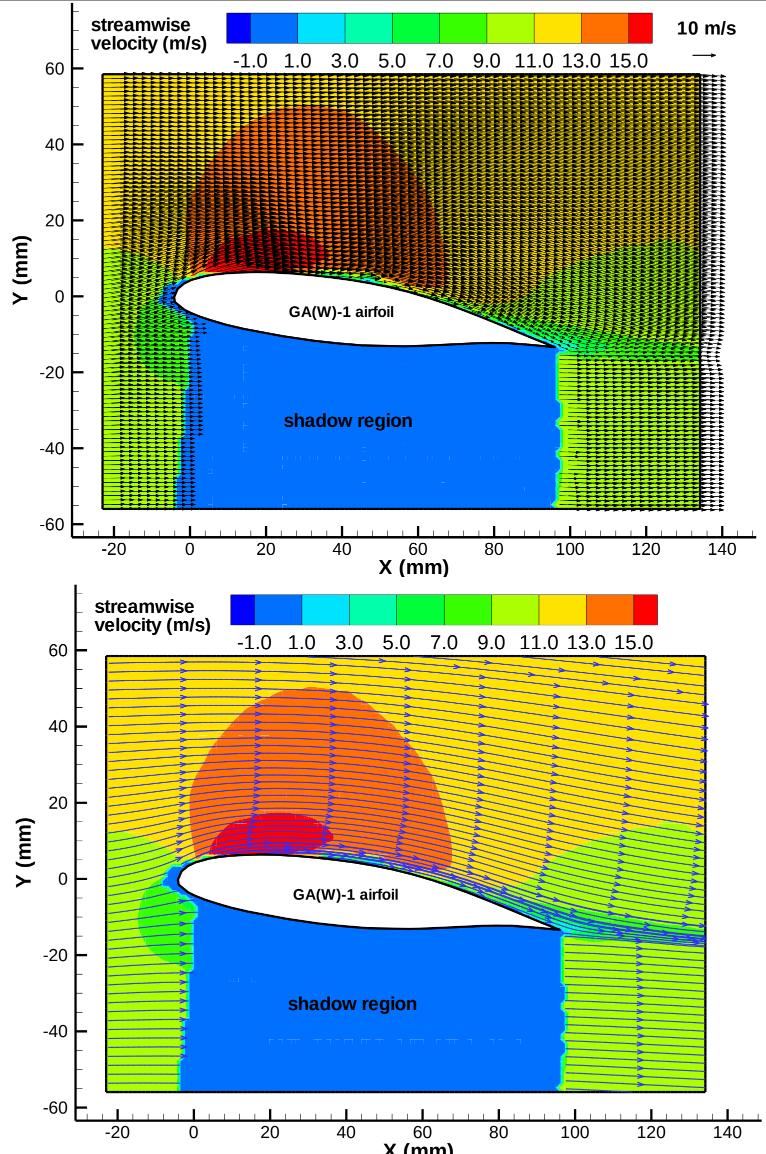

B. ensemble-averaged results

PIV Measurement Results

(AOA=10.0 degrees, Re=68,000, spatial resolution $\Delta/C \approx 0.04$)

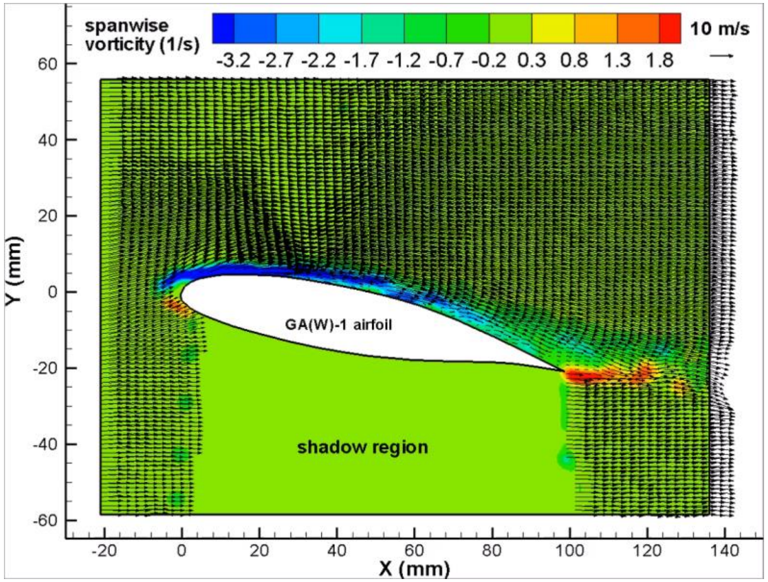

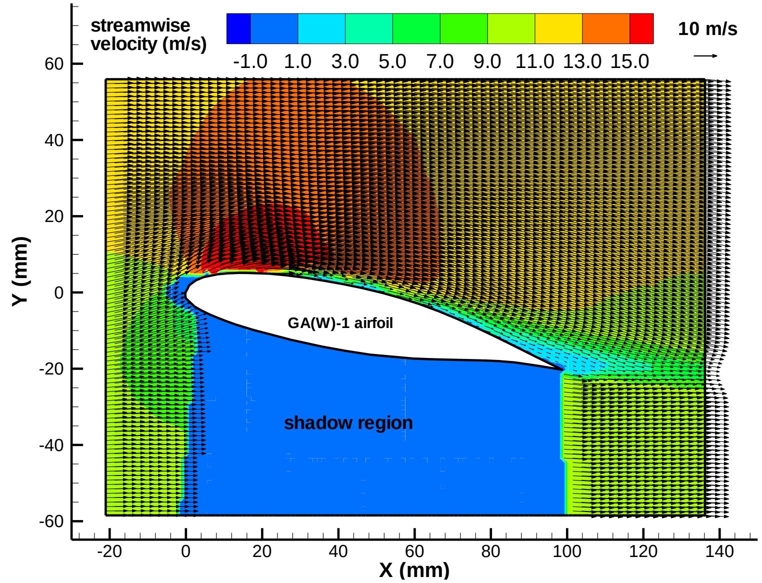

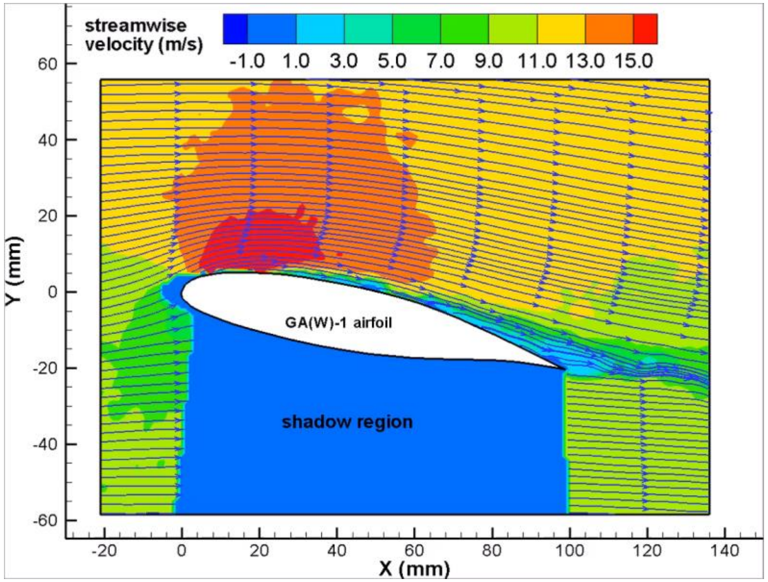

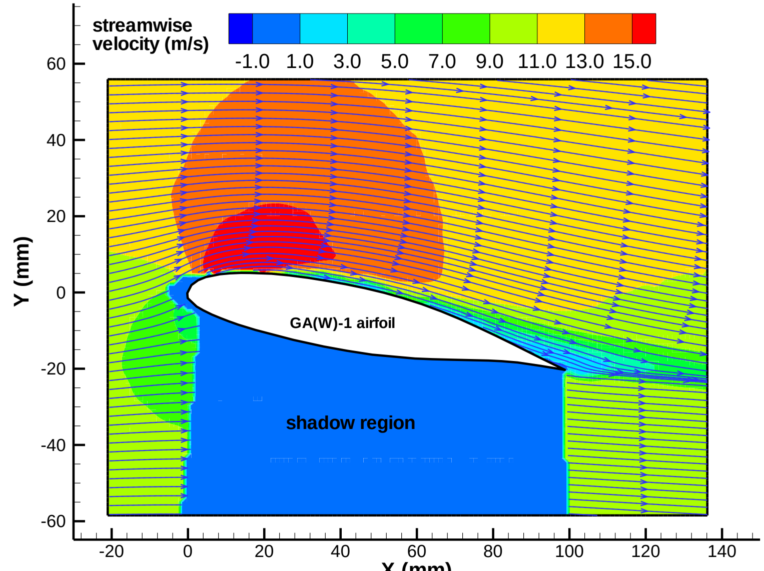

B. ensemble-averaged results

PIV Measurement Results

(AOA=12.0 degrees, Re=68,000, spatial resolution $\Delta/C \approx 0.04$)

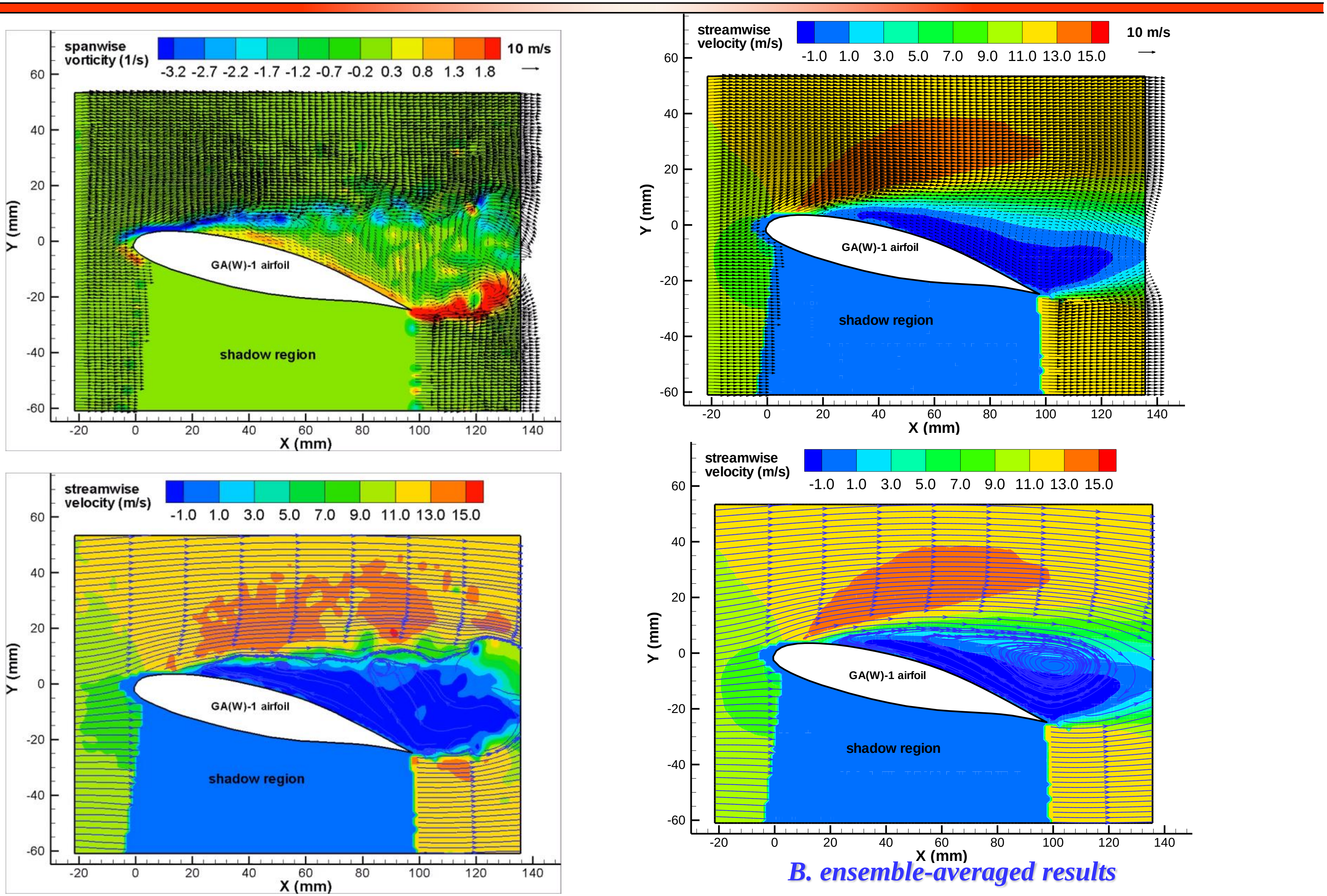

B. ensemble-averaged results

PIV Measurement Results

(AOA=6.0 degrees, Re=68,000, spatial resolution $\Delta/C \approx 0.01$)

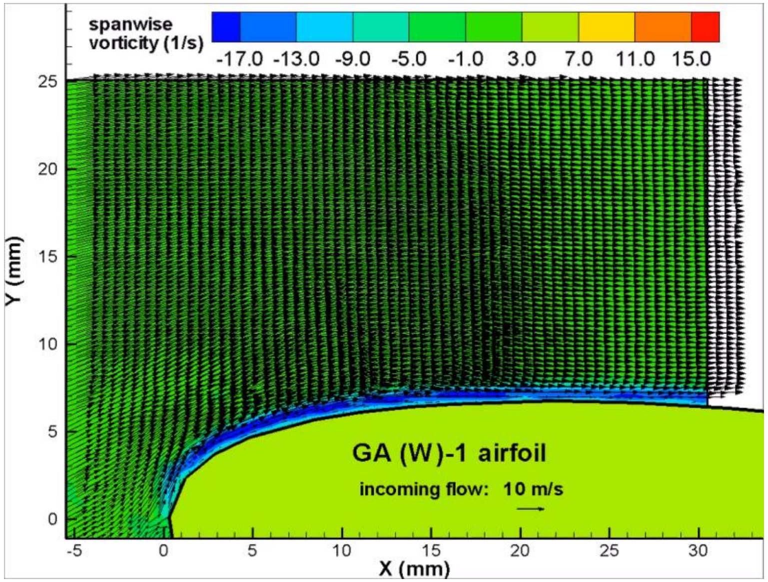

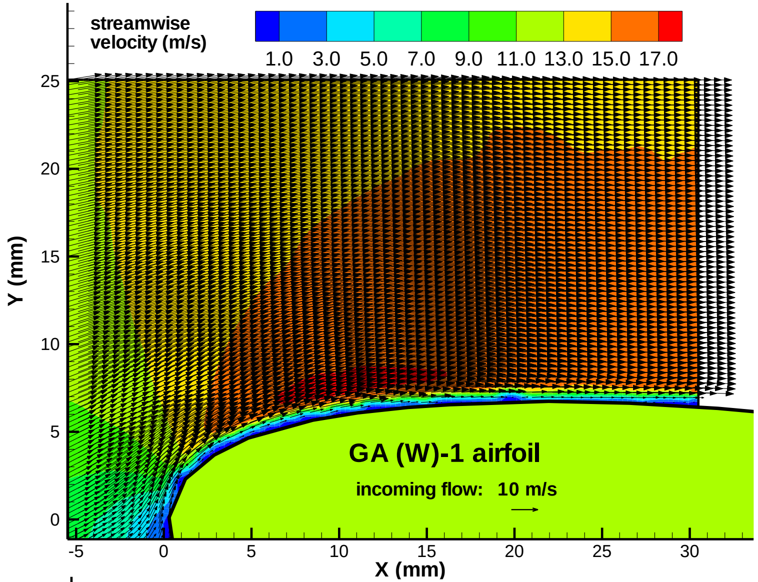

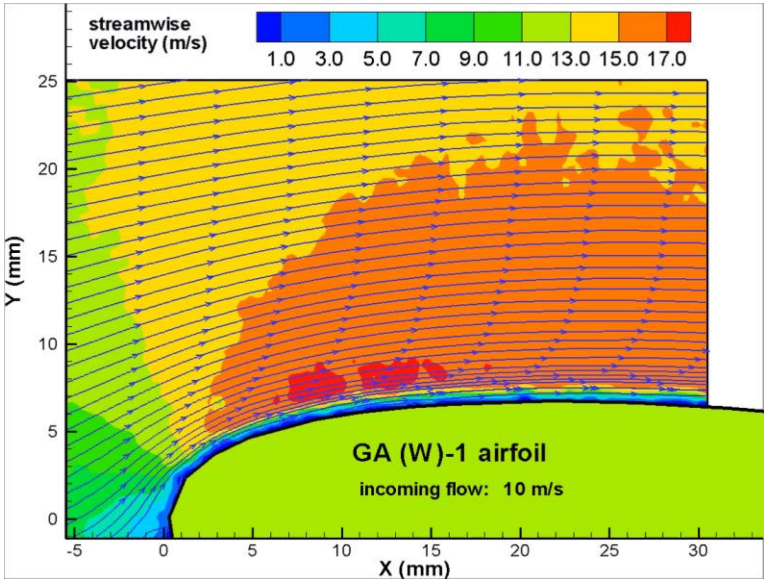

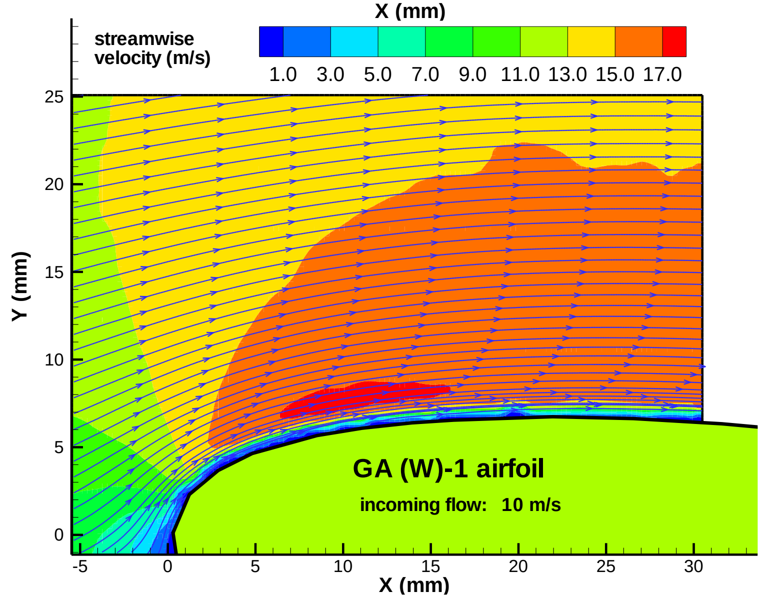

B. ensemble-averaged results

PIV Measurement Results

(AOA=10.0 degrees, Re=68,000, spatial resolution $\Delta/C \approx 0.01$)

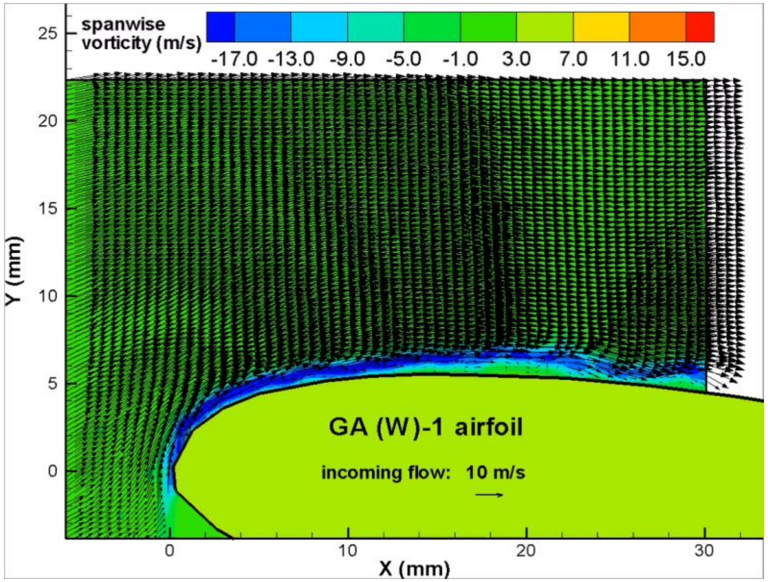

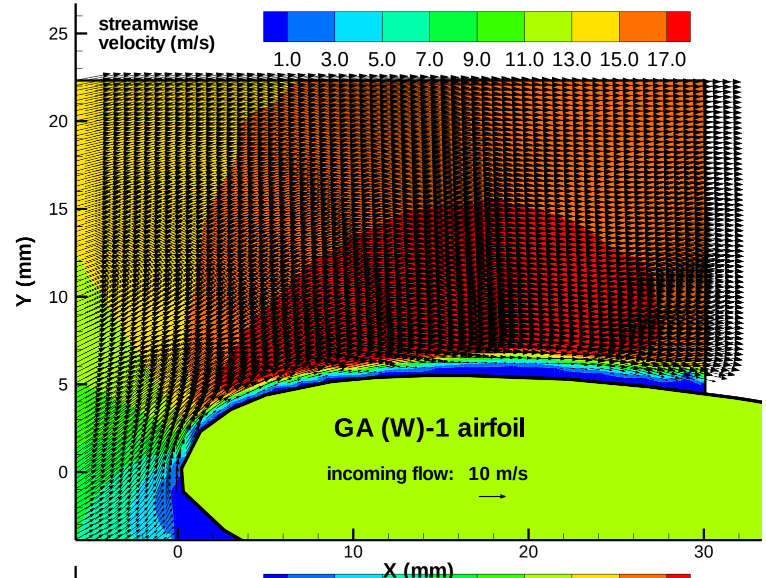

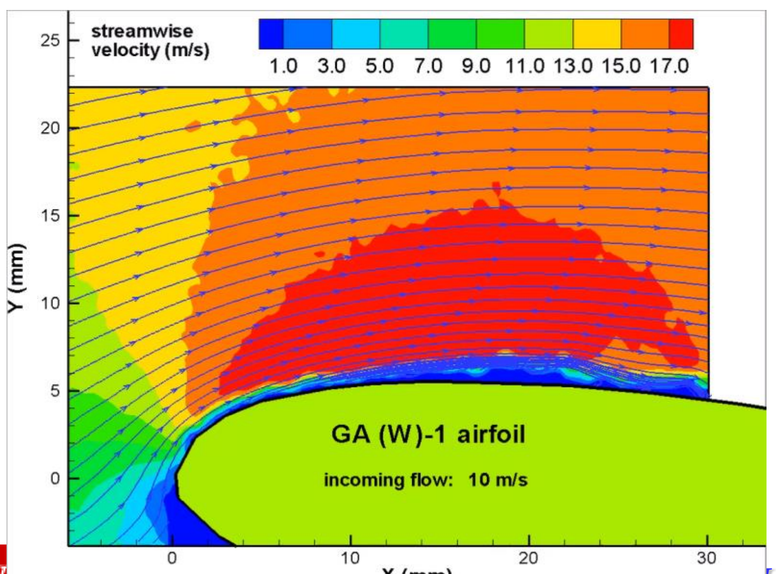

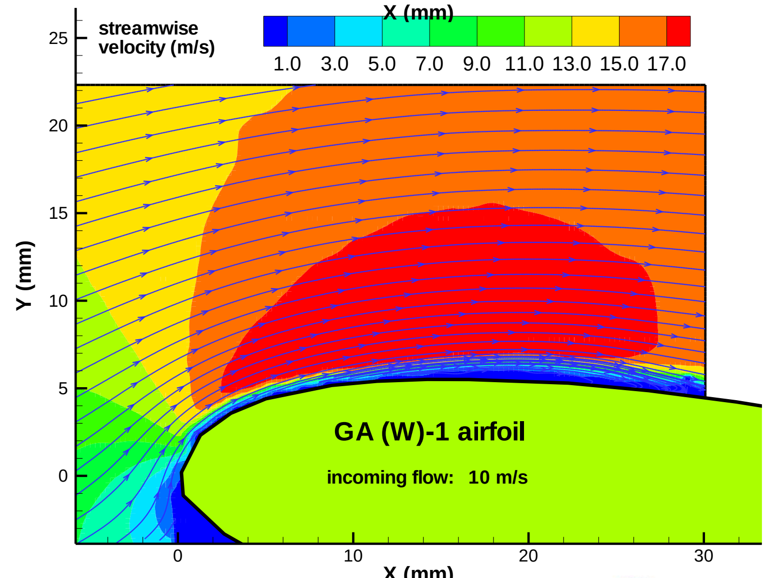

B. ensemble-averaged results

PIV Measurement Results

(AOA=12.0 degrees, Re=68,000, spatial resolution $\Delta/C \approx 0.01$)

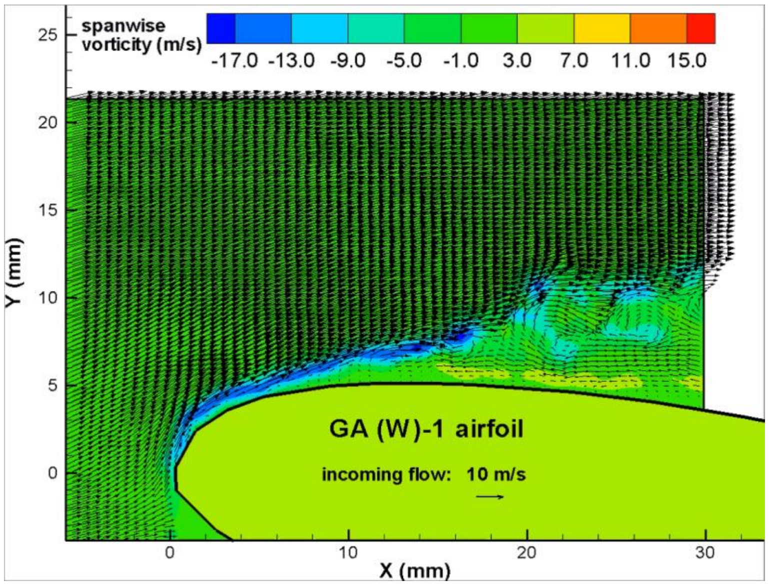

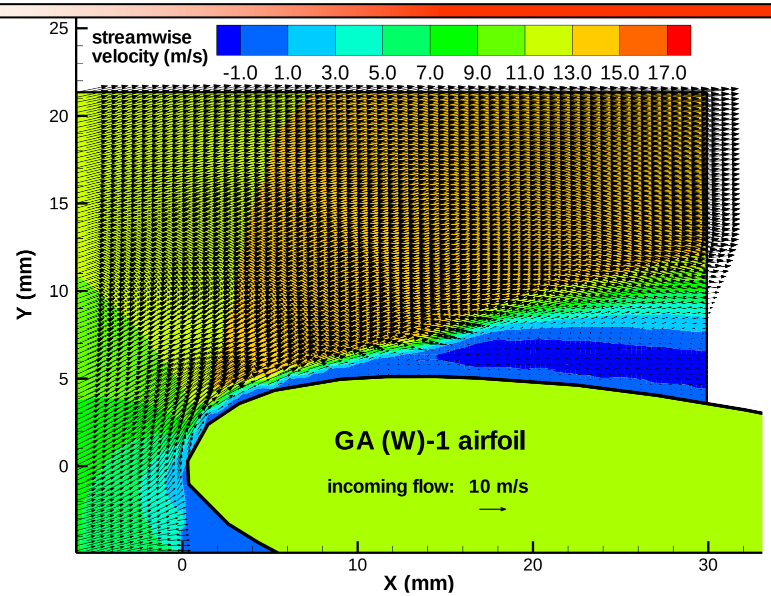

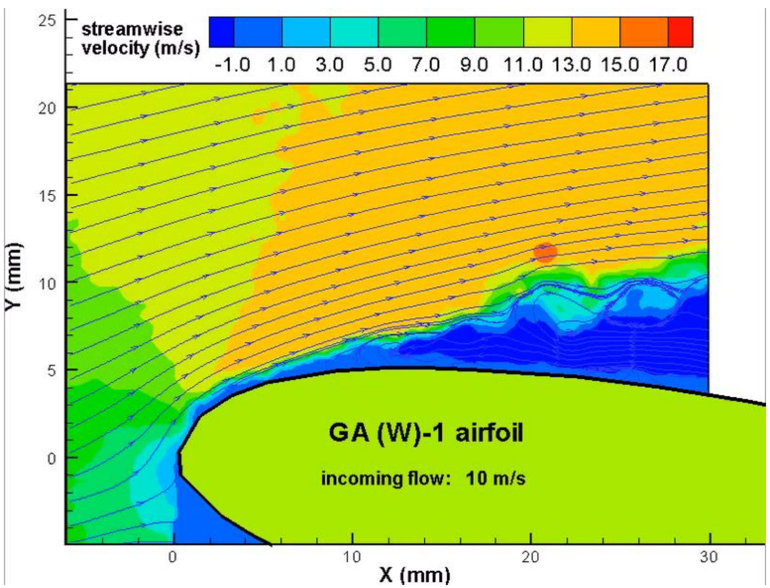

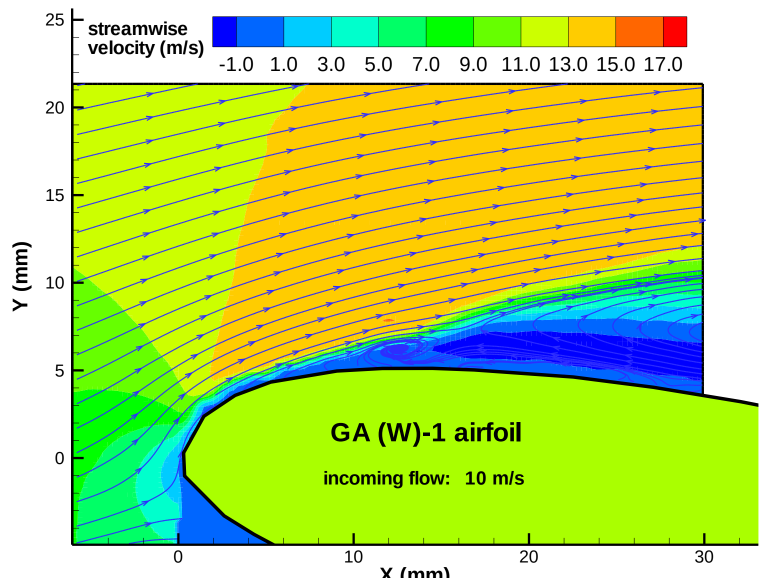

B. ensemble-averaged results

PIV Measurement Results

(AOA=10.0 degrees, Re=68,000, spatial resolution level 3)

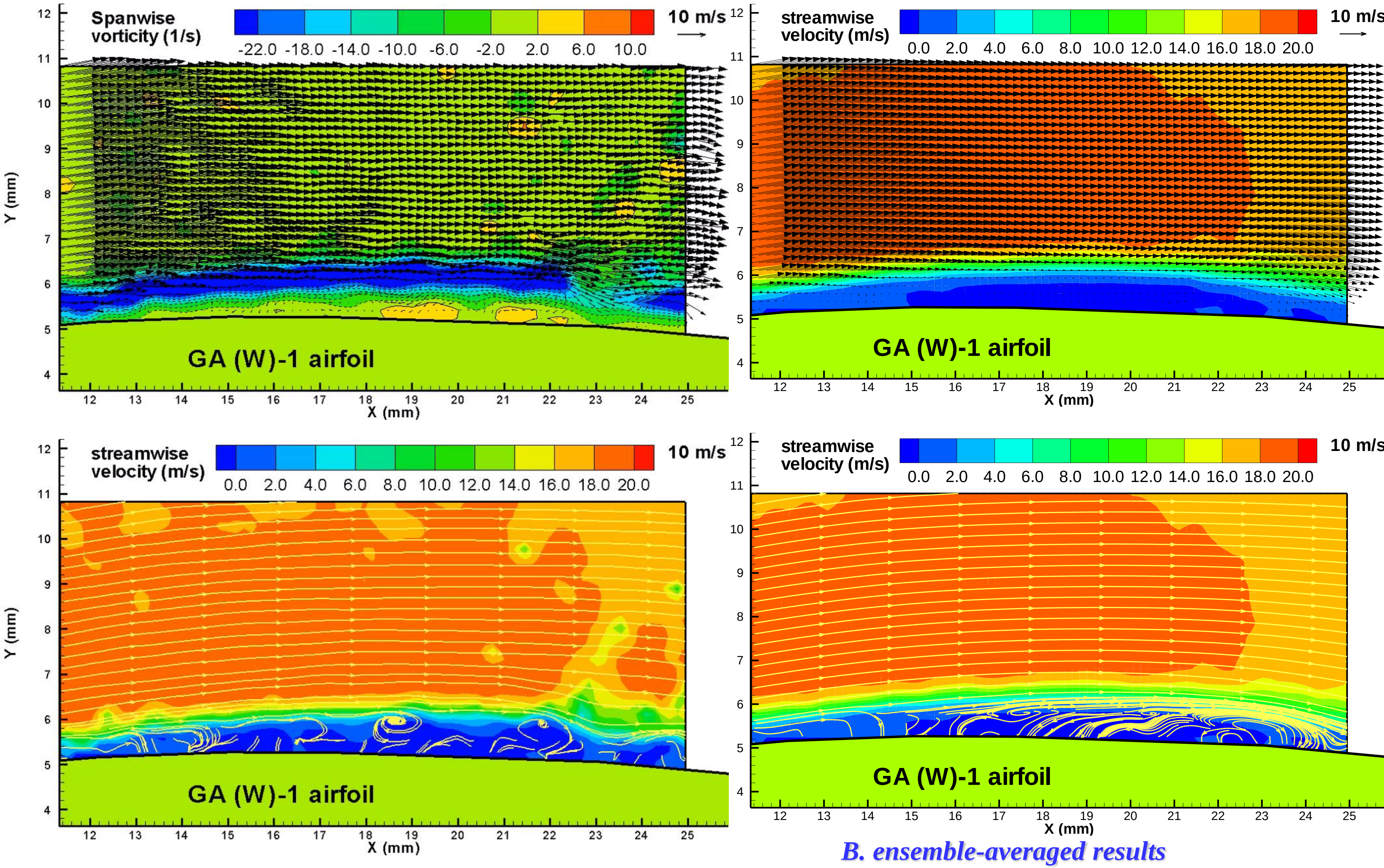

B. ensemble-averaged results

PIV Measurement Results
(AOA=10.0 degrees, Re=68,000, spatial resolution level 3)

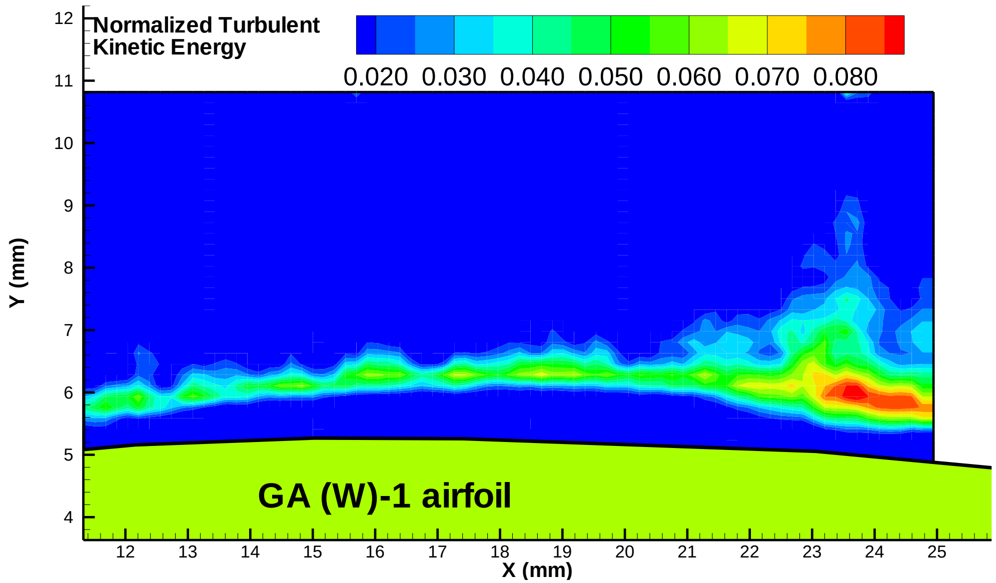

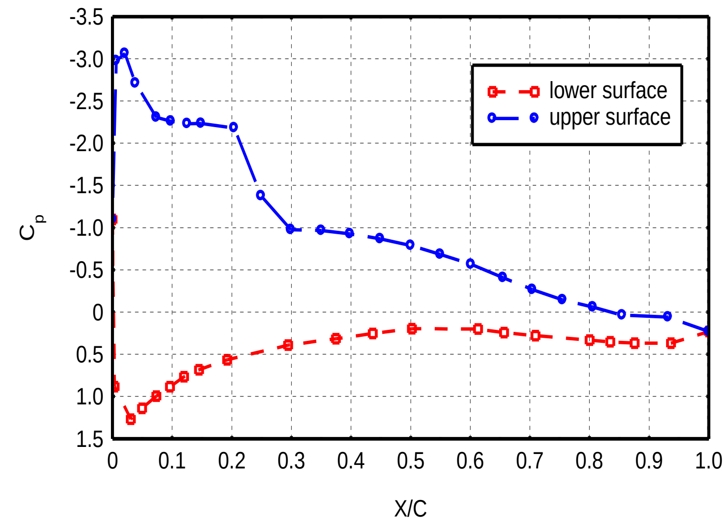

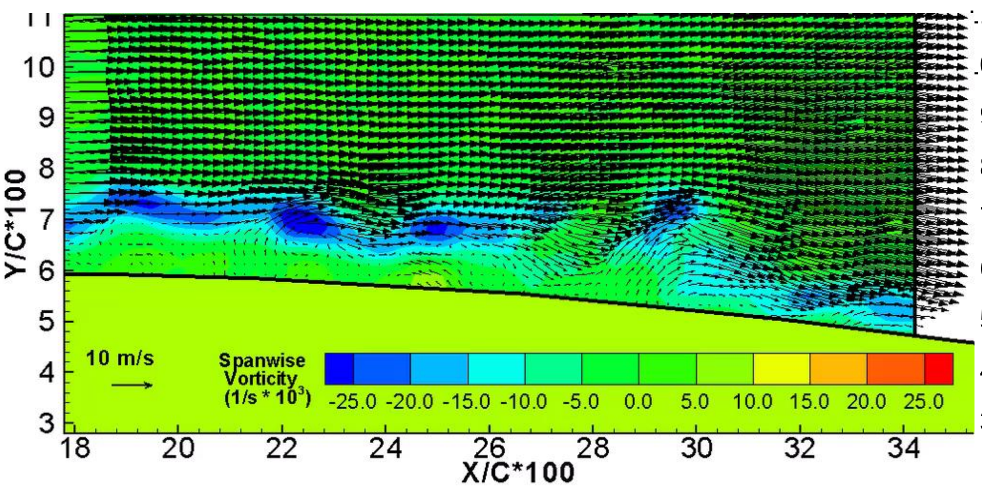

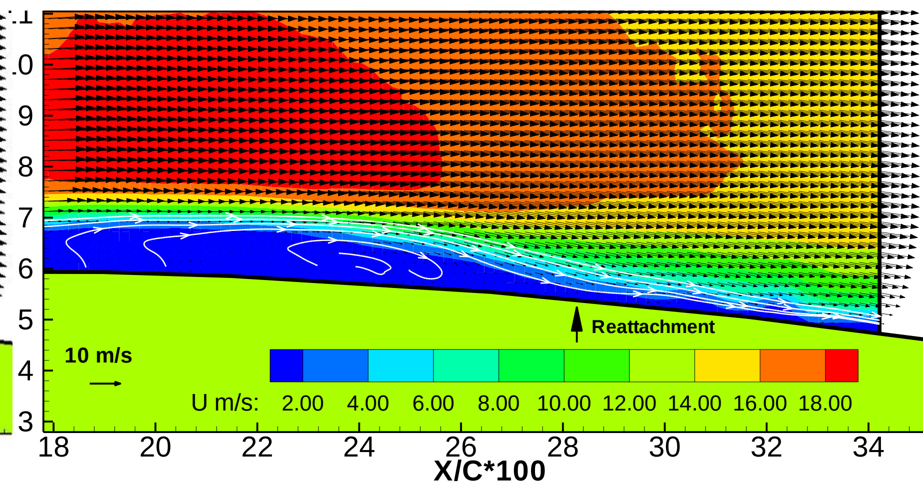

PIV measurement results at AOA = 10 deg, Re=68,000

(Hu et al., Journal of Fluid Engineering, 2009)

Aerodynamic Hysteresis Phenomena

- ***Hysteresis is the property of systems that do not instantly react to a change, or do not completely return to their original state.***
- ***The state of such a system usually depends on its immediate history.***
- ***Aerodynamic hysteresis of an airfoil refers to the aerodynamic characteristics becomes history dependent, i.e., dependent on the sense of change of the angle of attack, near the airfoil stall angle.***
- ***Hysteresis phenomena have been found to be relatively common for round nosed airfoils at low Reynolds numbers.***

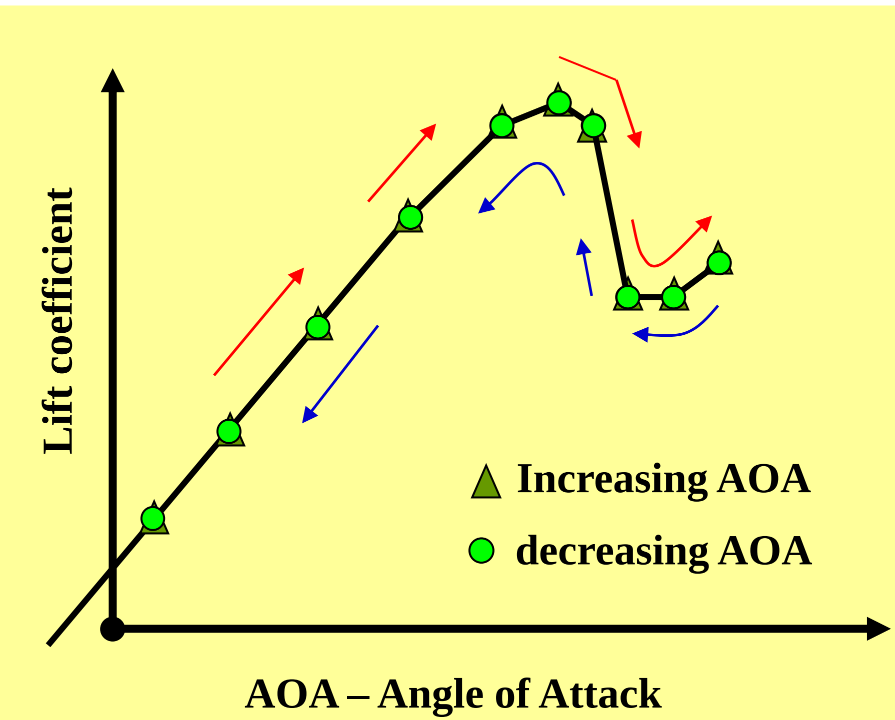

Lift coefficient curve of a "typical" airfoil

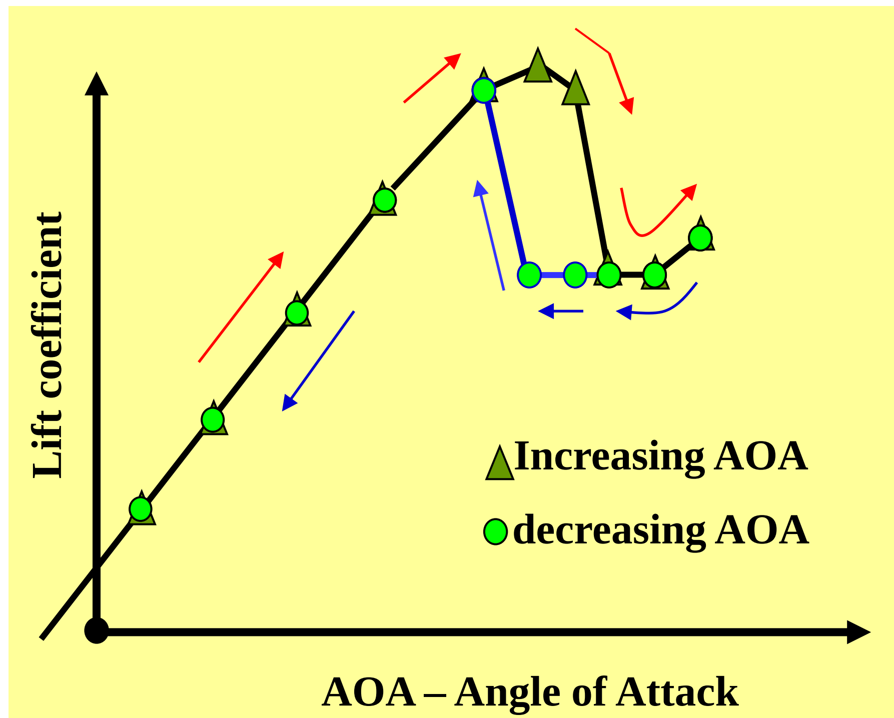

Lift coefficient curve with hysteresis

Measured airfoil lift and drag coefficient profiles

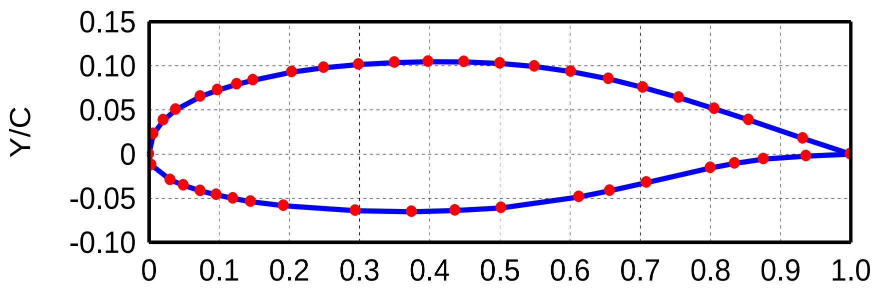

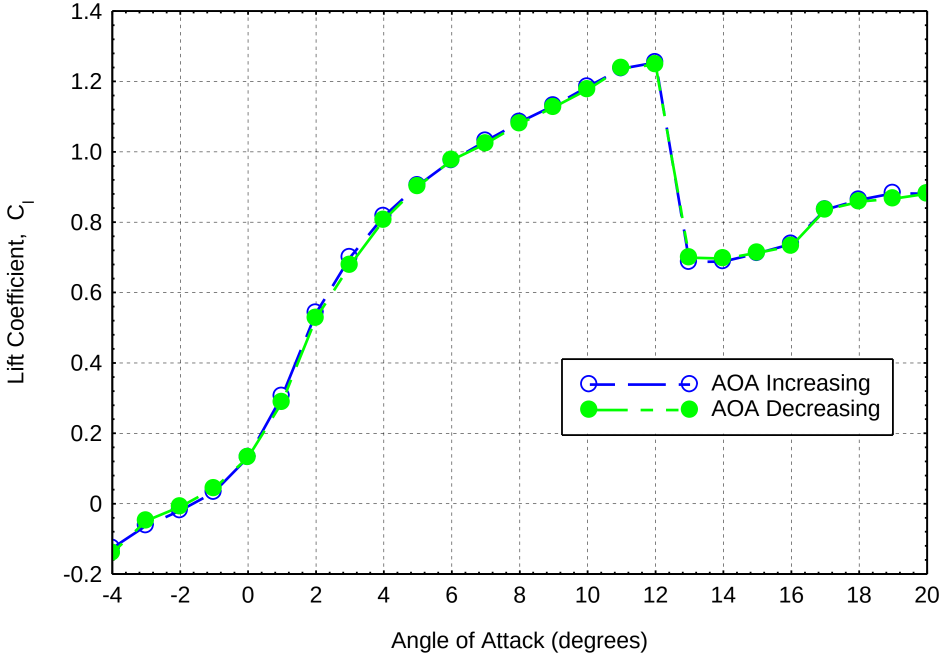

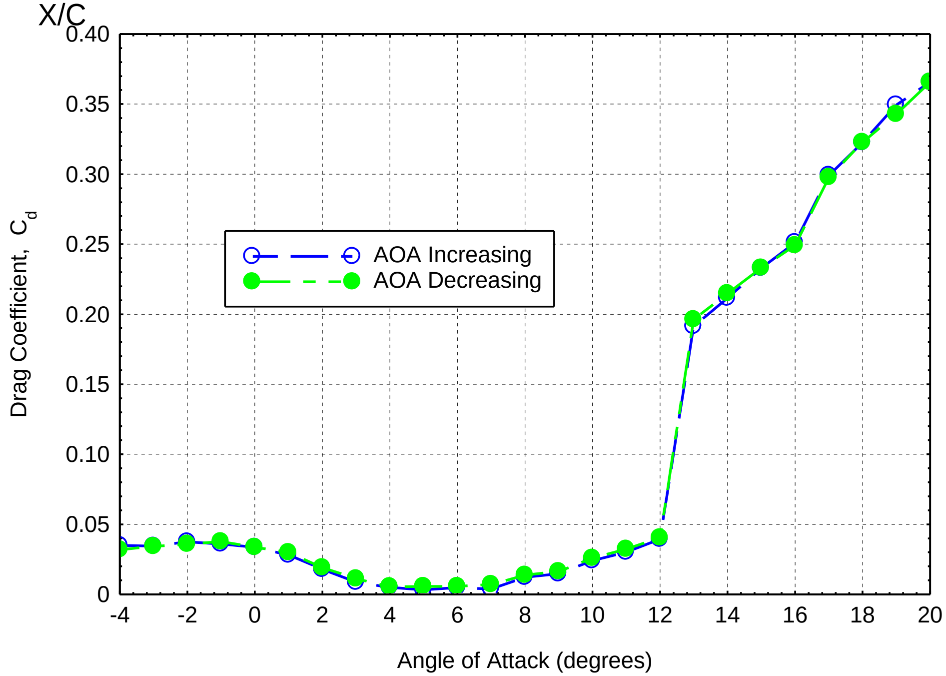

Lift coefficient vs. AOA

Drag coefficient vs. AOA

$Re_C = 100{,}000$.

The turbulence intensity of the incoming streams: ~1.0%

Measured airfoil lift and drag coefficient profiles

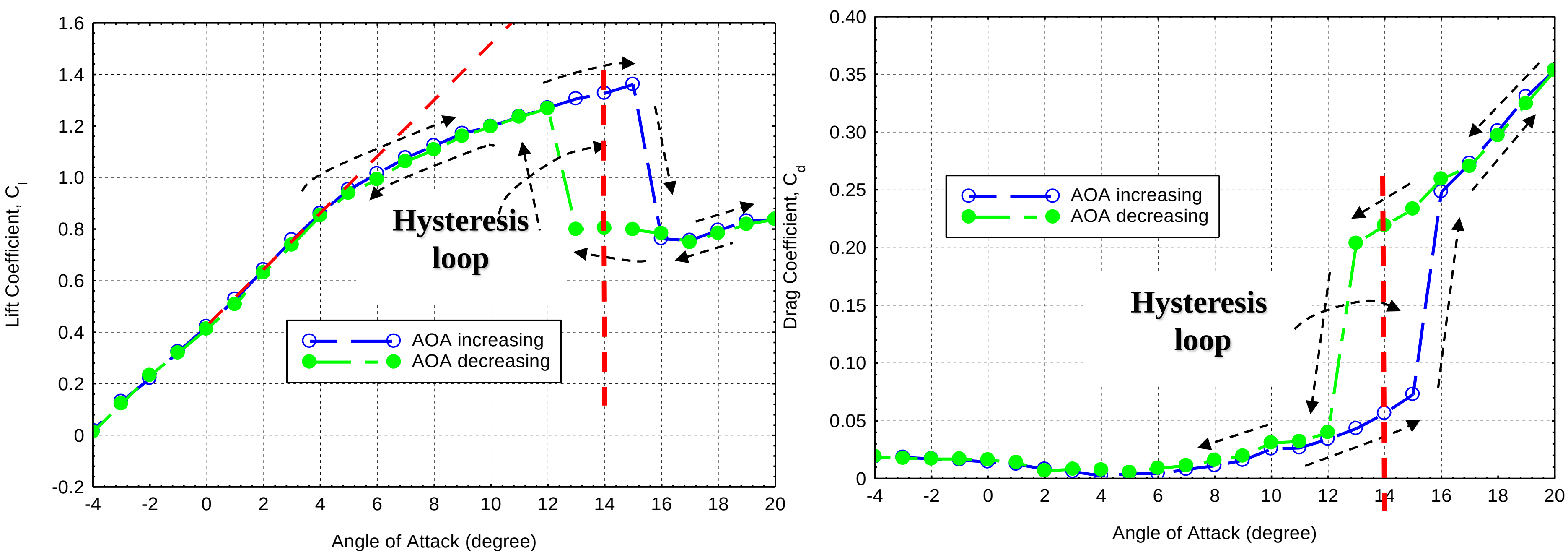

$Re_C = 160{,}000$

- *The hysteresis loop was found to be clockwise in the lift coefficient profiles, and counter-clockwise in the drag coefficient profiles.*
- *The aerodynamic hysteresis resulted in significant variations of lift coefficient, C_l, and lift-to-drag ratio, l/d, for the airfoil at a given angle of attack.*
- *The lift coefficient and lift-to-drag ratio at AOA = 14.0 degrees were found to be C_l = 1.33 and l/d = 23.5 when the angle is at the increasing angle branch of the hysteresis loop.*
- *The values were found to become C_l = 0.8 and l/d = 3.66 for the same AOA=14.0 degrees when the angle is at the deceasing angle branch of the hysteresis loop*

Measured airfoil lift and drag coefficient profiles

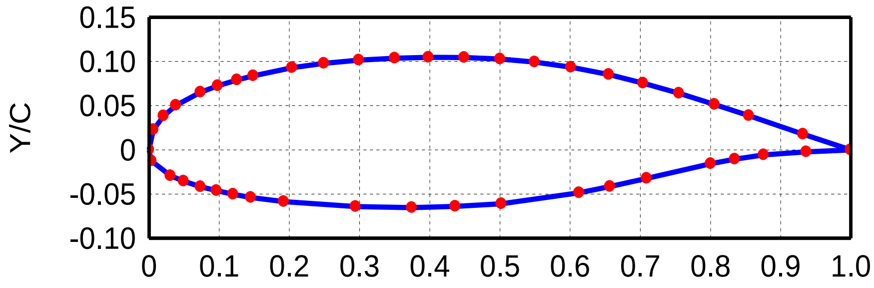

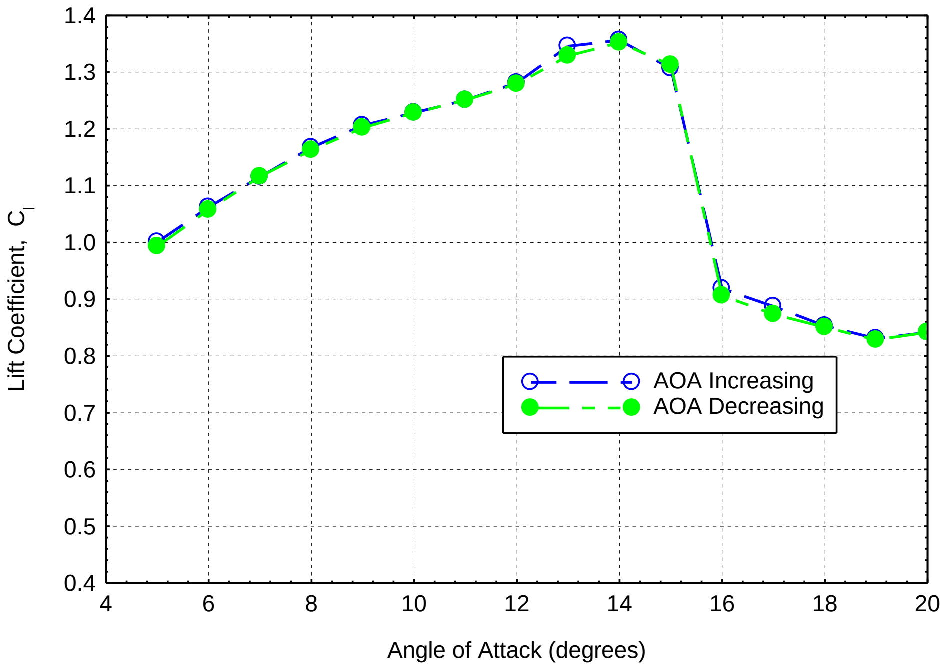

Lift coefficient vs. AOA

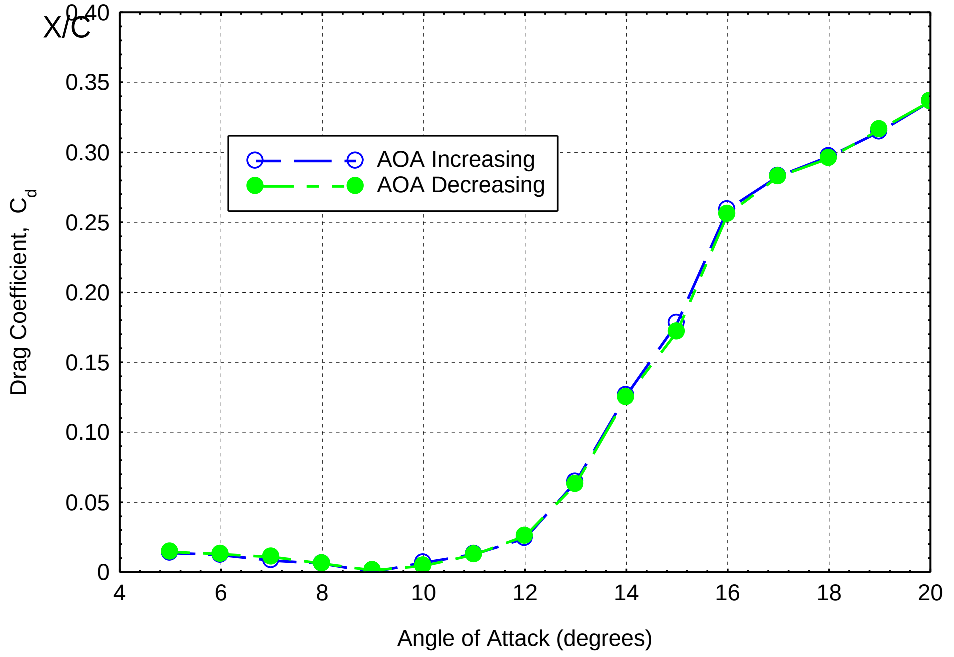

Drag coefficient vs. AOA

Re_C = 400,000.

The turbulence intensity of the incoming streams: ~1.0%

Measured surface pressure distribution around the airfoil

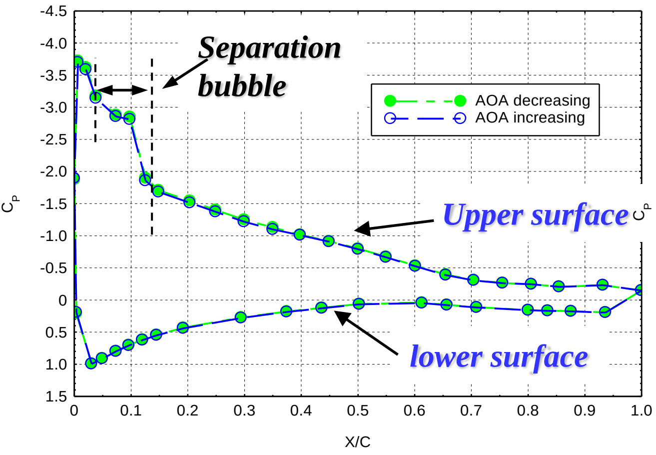

AOA =12.0 degrees

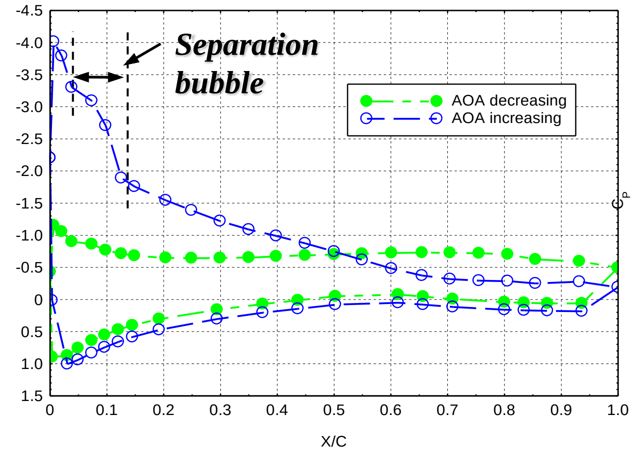

AOA =13.0 degrees

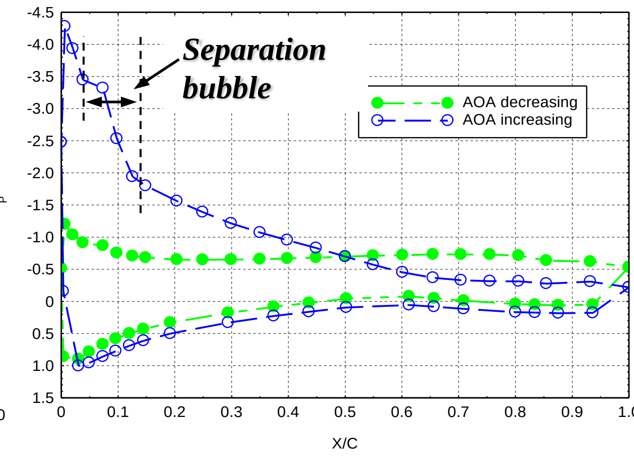

AOA =14.0 degrees

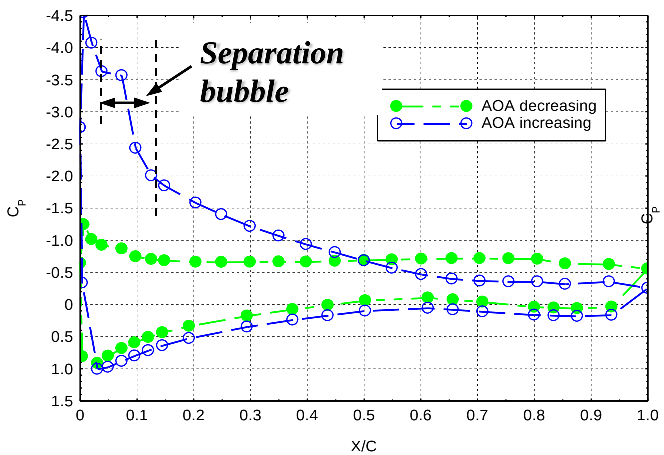

AOA =15.0 degrees

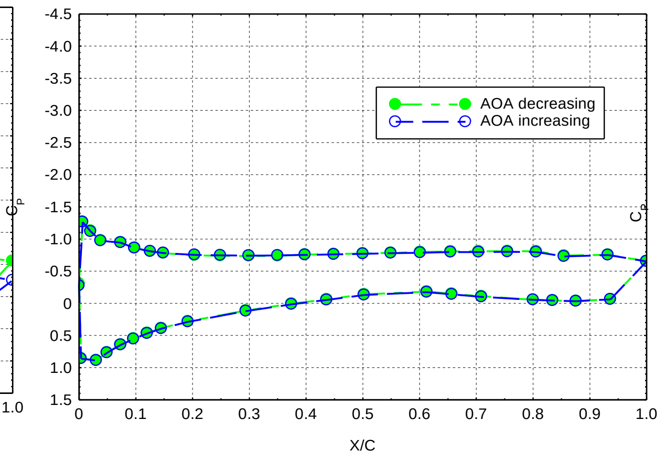

AOA =16.0 degrees

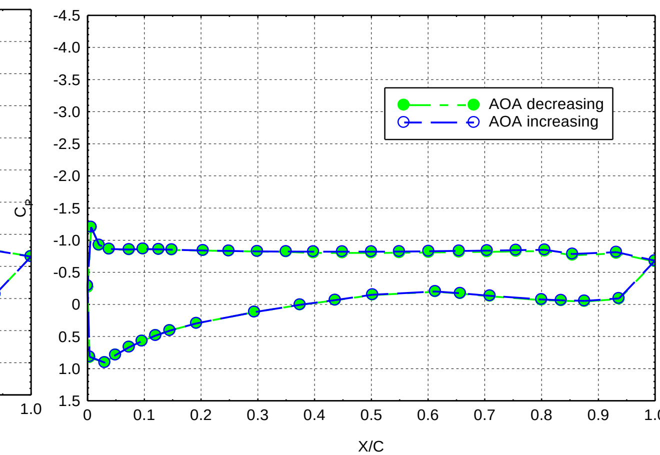

AOA =17.0 degrees

U_∞ = 24 m/s, Re_C = 160,000.

The turbulence intensity of the incoming streams: ~1.0%

Measured Surface Pressure Distribution at AOA=14.0 Deg

- ***Based in the measured surface pressure distribution, the separation, transition, and reattachment points at AOA=12.0 ~ 15.0 degrees were estimated to locate at X/C ≈0.05, X/C ≈ 0.08 and X/C ≈ 0.15 respectively.***
- ***The length of the laminar separation bubble (i.e., the distance between the separation and reattachment points) was found to be ~ 10 % of the airfoil chord length, which is almost independent of the angle of attack.***

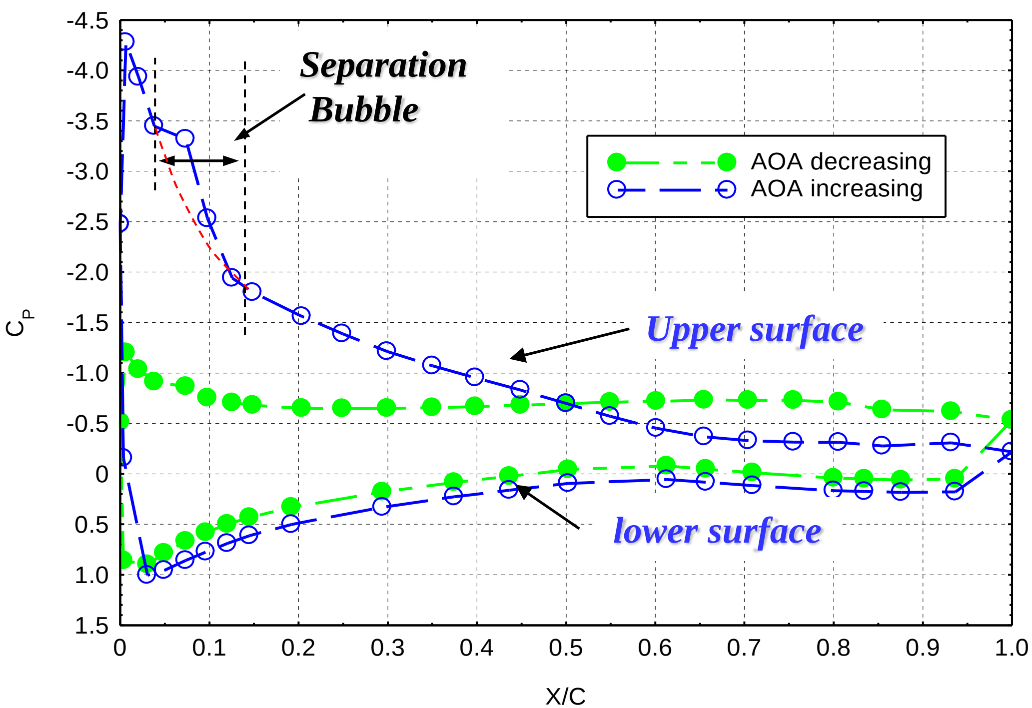

Measured Surface Pressure Distribution at AOA=14.0 degrees

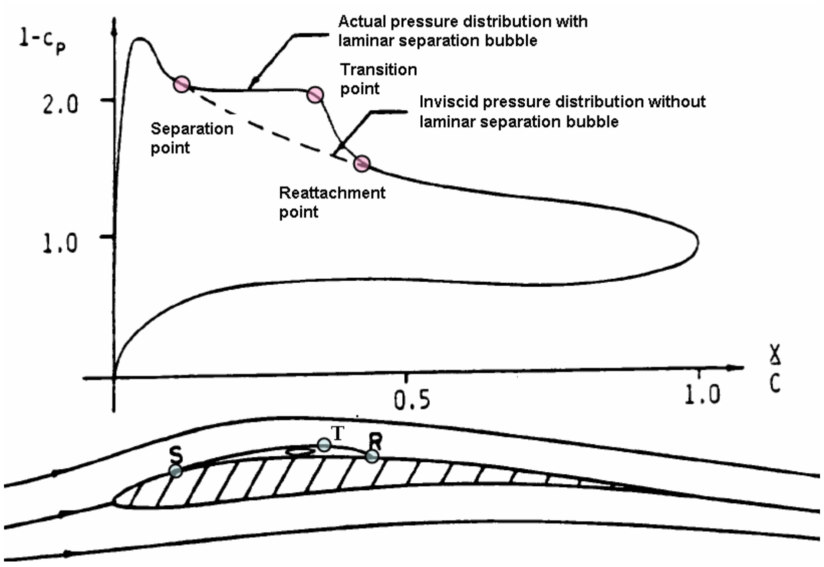

Typical surface pressure distribution when a laminar separation bubble is formed (Russell, 1979)

Experimental Setup for PIV Measurements

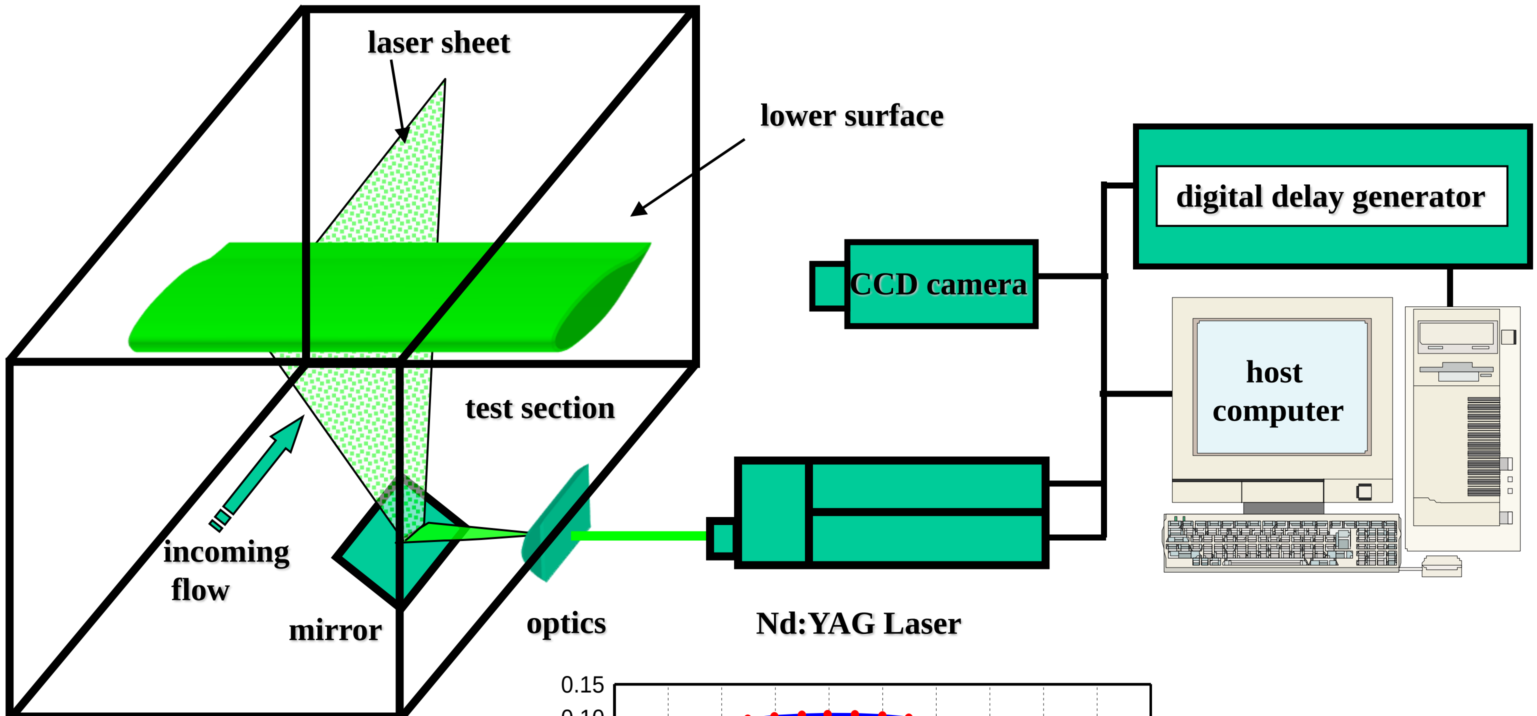

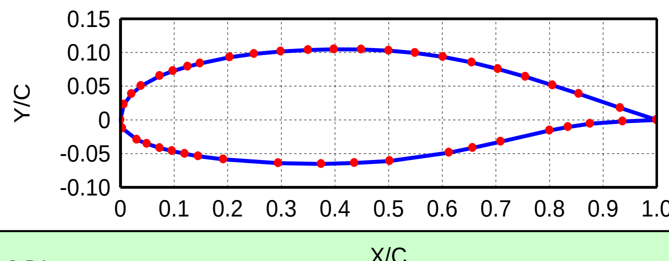

Experimental conditions:

Incoming flow velocity: $U_{\infty} = 24.0 \ m/s, \quad \mathrm{Re}_C = 160{,}000$

Turbulent intensity: $\sim 1.0\%$

Angle of Attack: $\alpha = -4.0^o \sim 20.0^o$

Two Spatial Resolution Levels for the PIV Measurements

Level 1:

A coarse level to study the global features of the flow structures around the airfoil.

Measurement window size: 160mm×140mm

Effective resolution: Δ/C = 0.018

Level 2:

A refined level to investigate the detailed features of the laminar boundary layer near the nose of the airfoil.

Measurement window size: 40mm × 30mm

Effective resolution: Δ/C = 0.0046

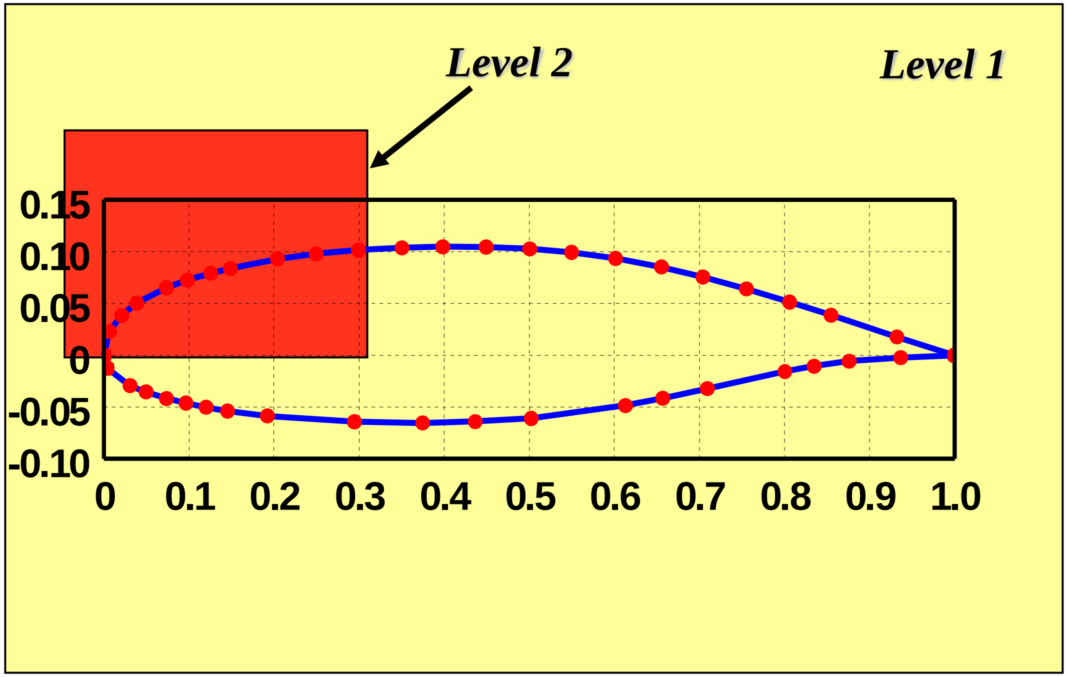

PIV Measurement results

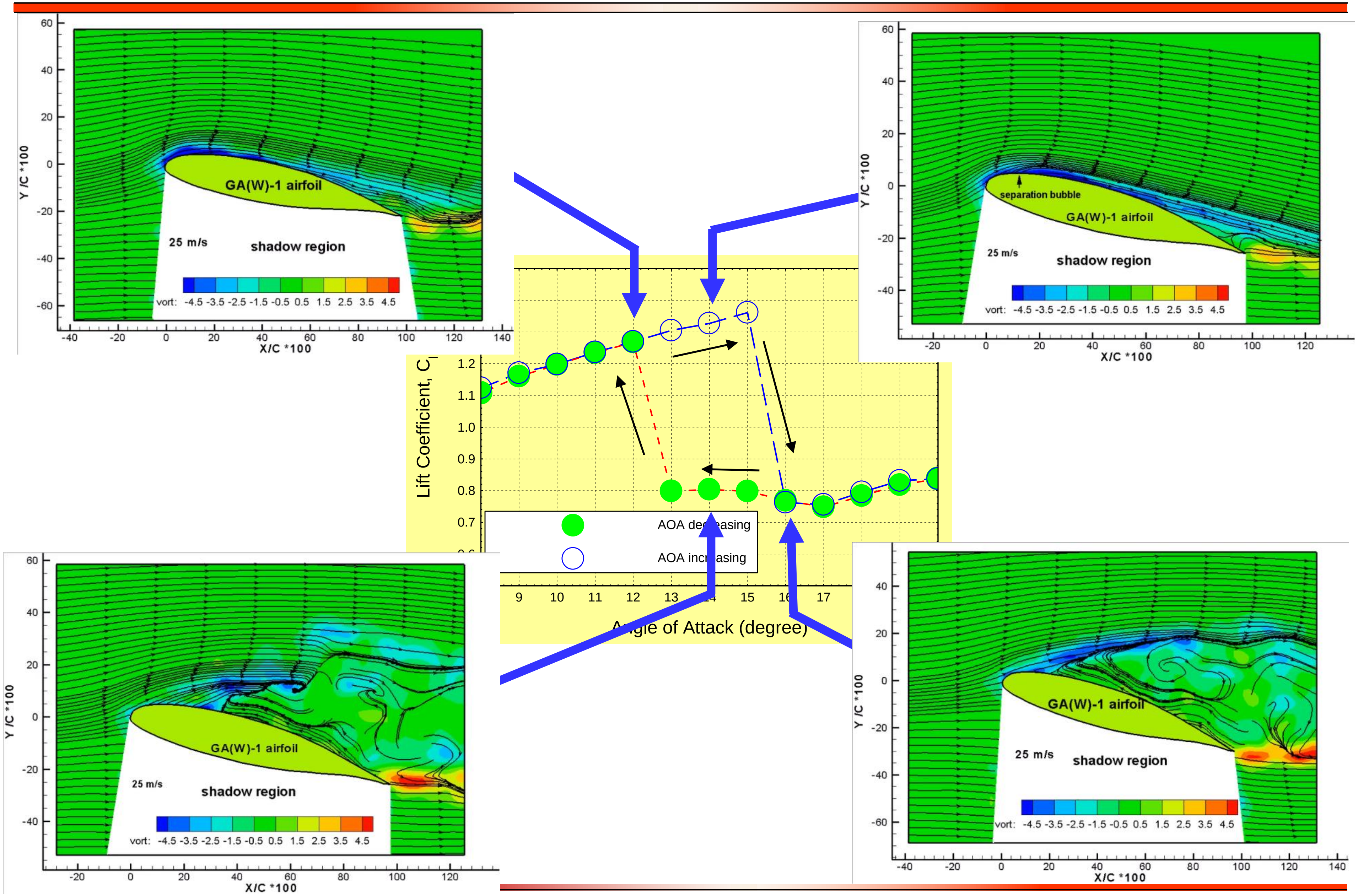

PIV Measurement results

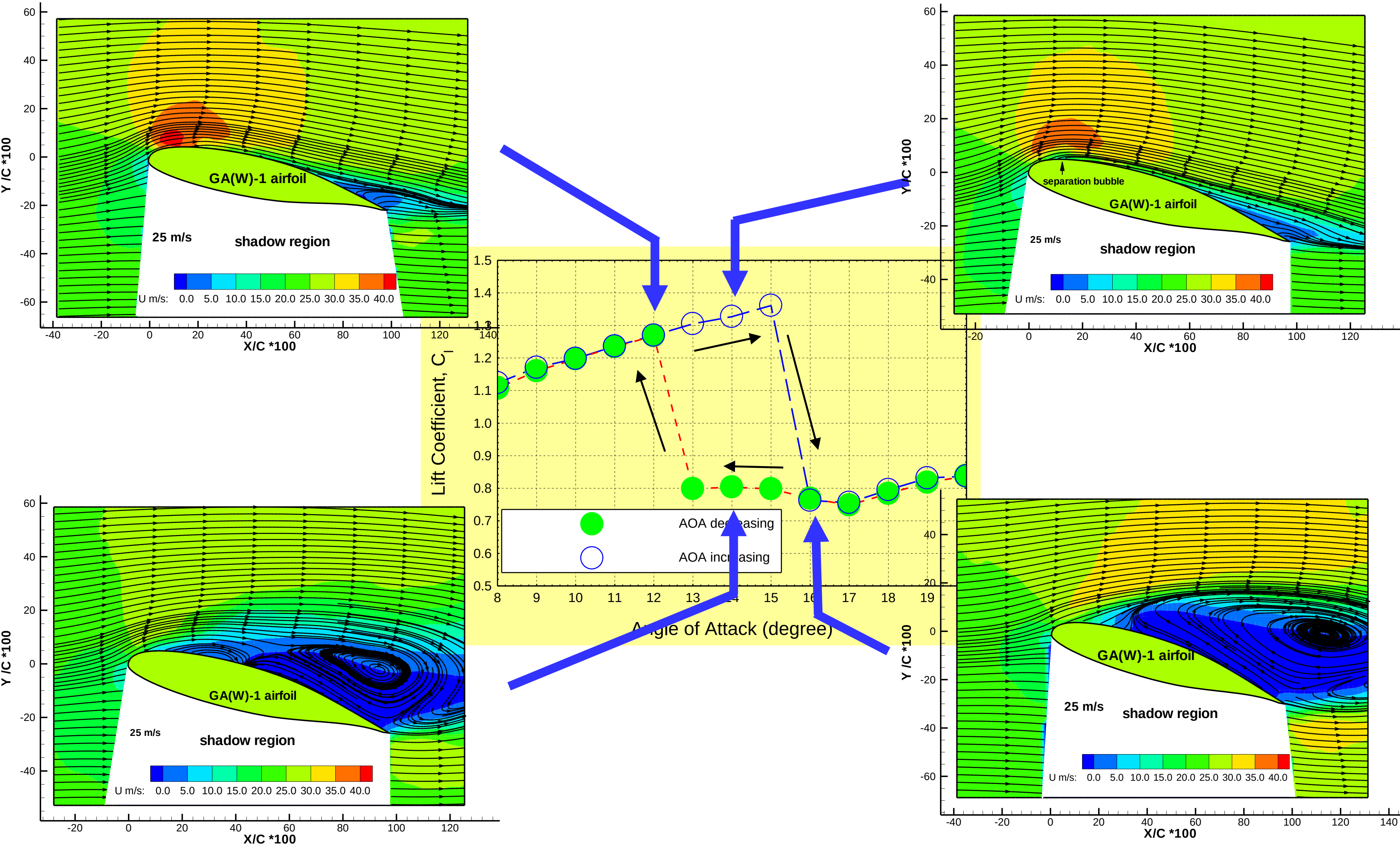

Measured Turbulence Kinetic Energy Distributions

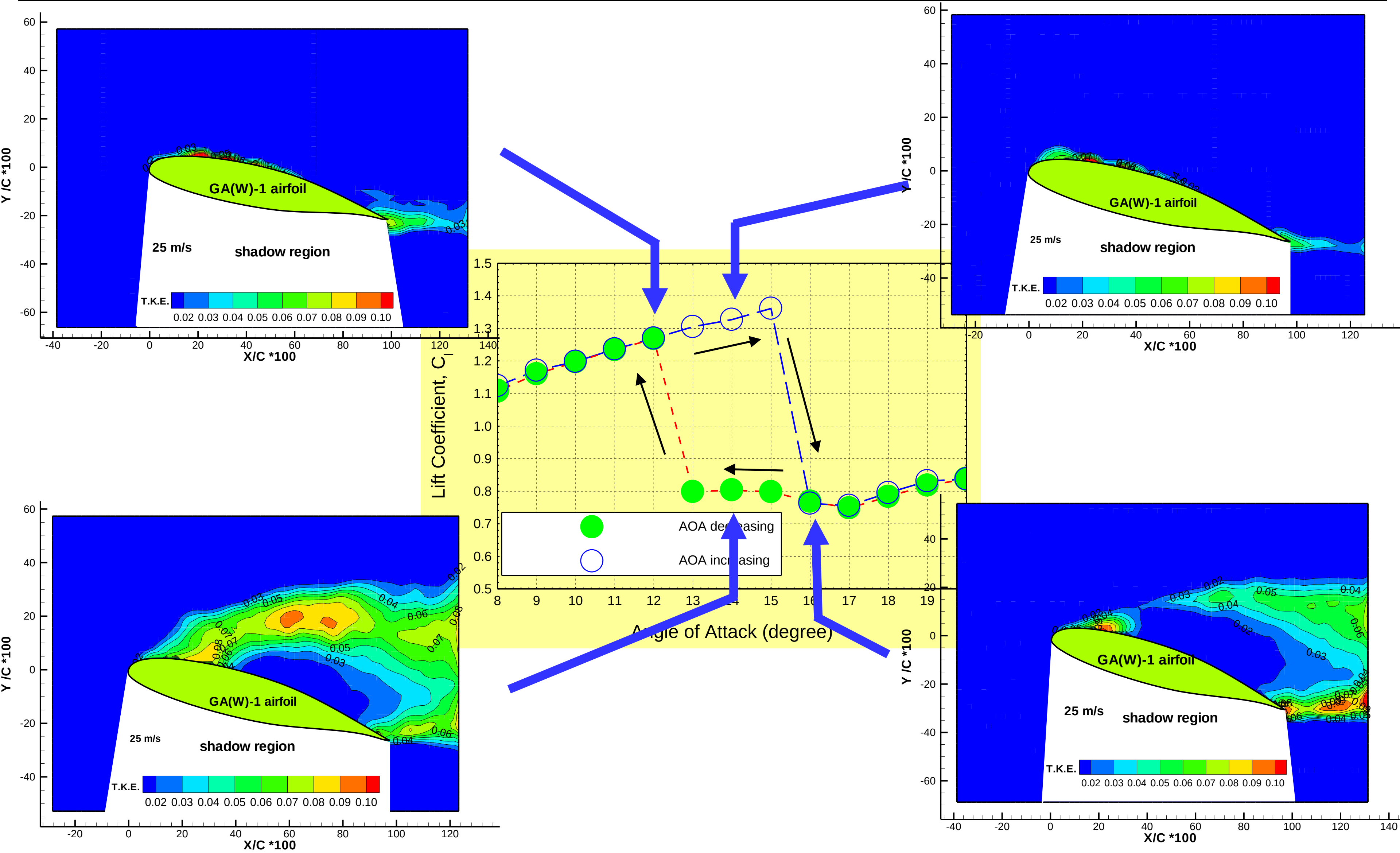

Refined PIV Measurement Results

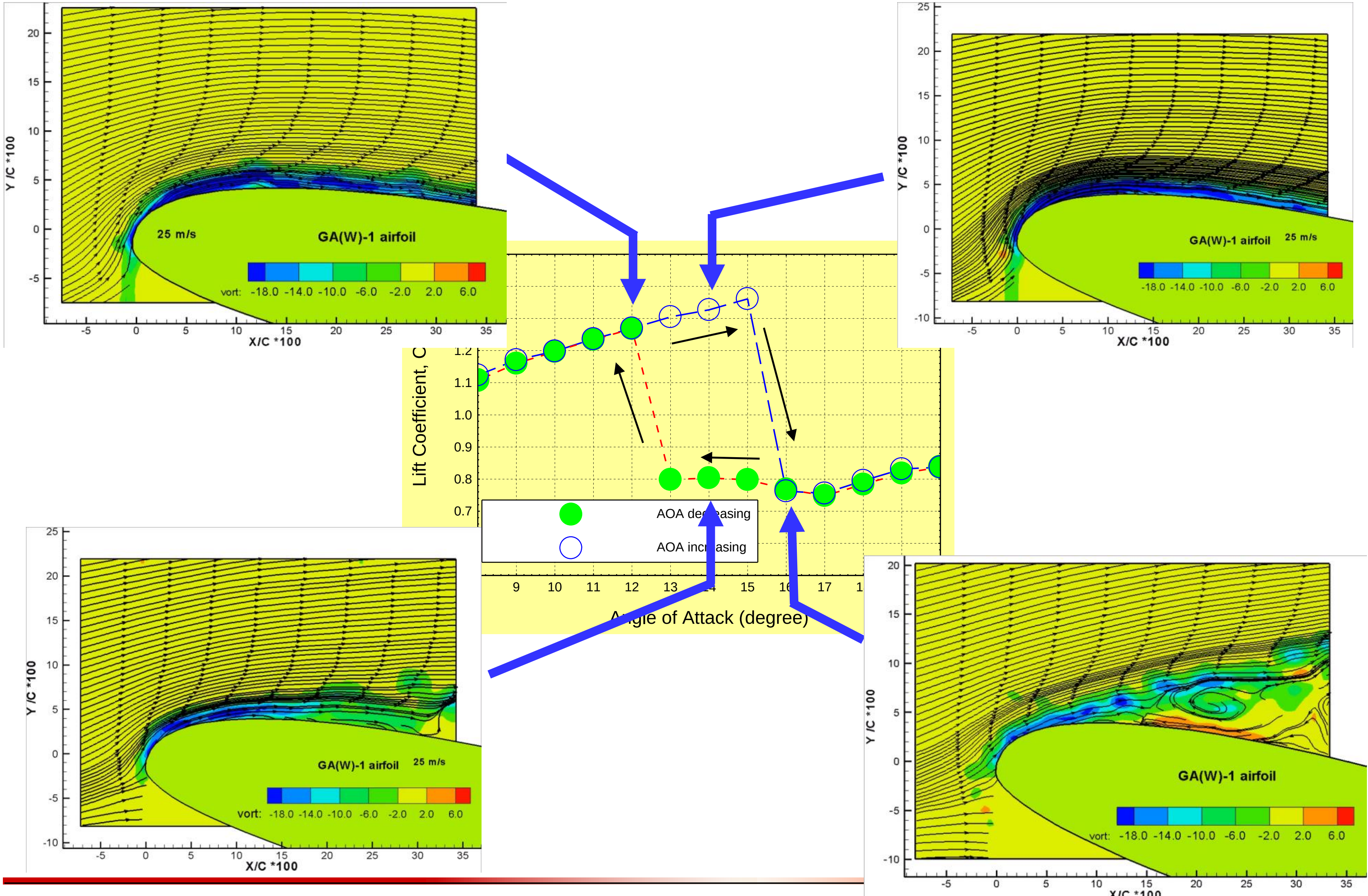

Refined PIV Measurement Results

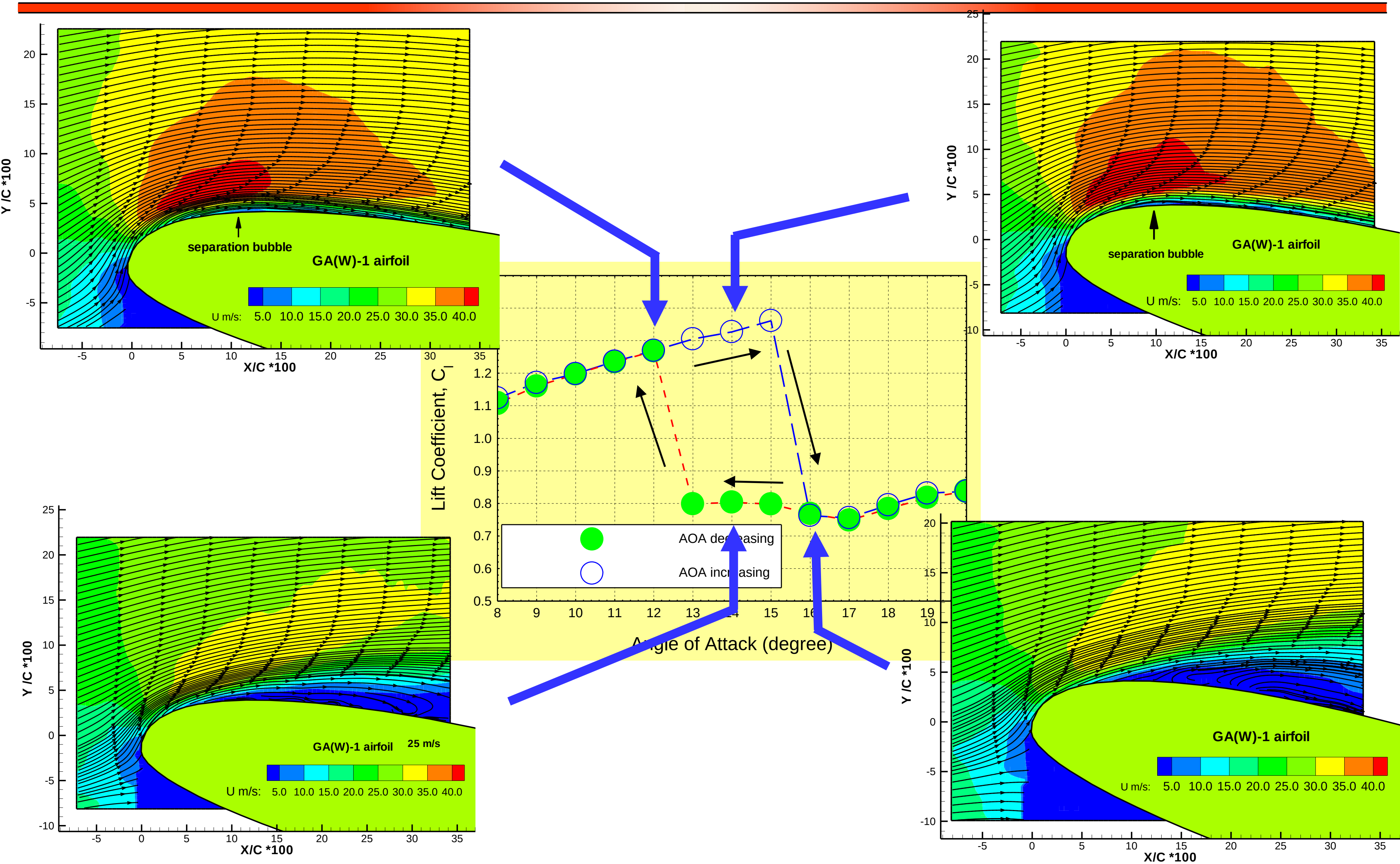

Active Flow Control of Airfoil Stall by Using an Oscillating Bubble Burst Plate

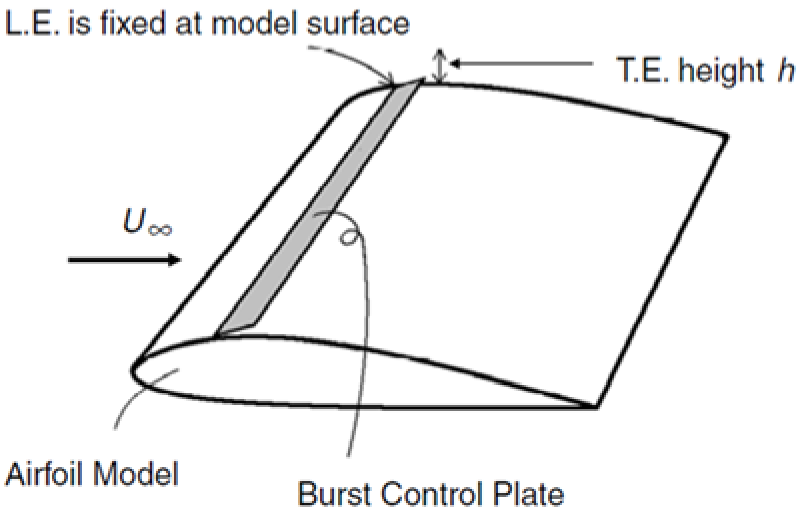

Active Flow Control on a Low-Reynolds Number Airfoil by Using an Oscillating Bubble Burst Plate

- *Rinoie, Okuno, and Sunada, 2009, "Airfoil Stall Suppression by Use of a Bubble Burst Control Plate", AIAA Journal Vol. 47, No. 2, 2009*

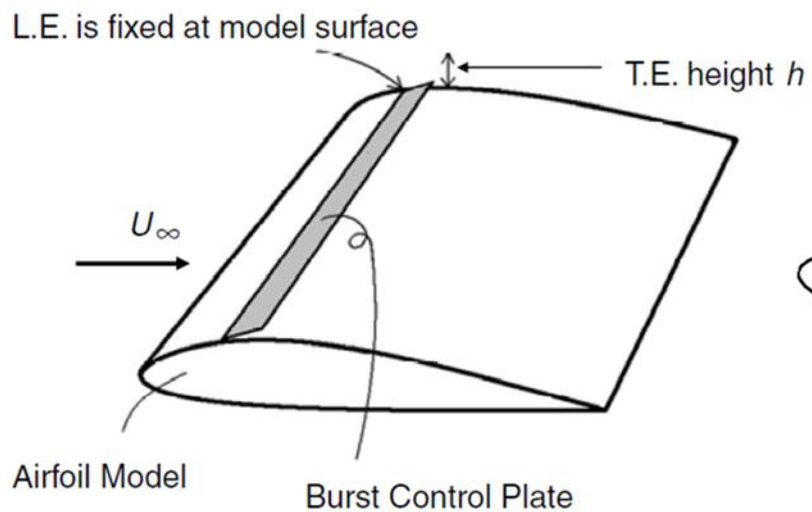

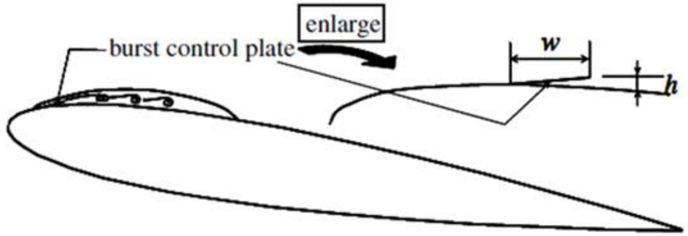

Findings

- Plate must be placed ahead of 10% chord
- Height greatly effects performance
- Delays stall by 2 degrees on NACA 0012
- Max lift coefficient increased by 0.1

Will A Dynamic Burst Control Plate Improve Performance?

Active Control of Laminar Separation Bubble

NACA 0012 Airfoil

- **300 mm Chord**
- **Span-wise Burst Control Plate**

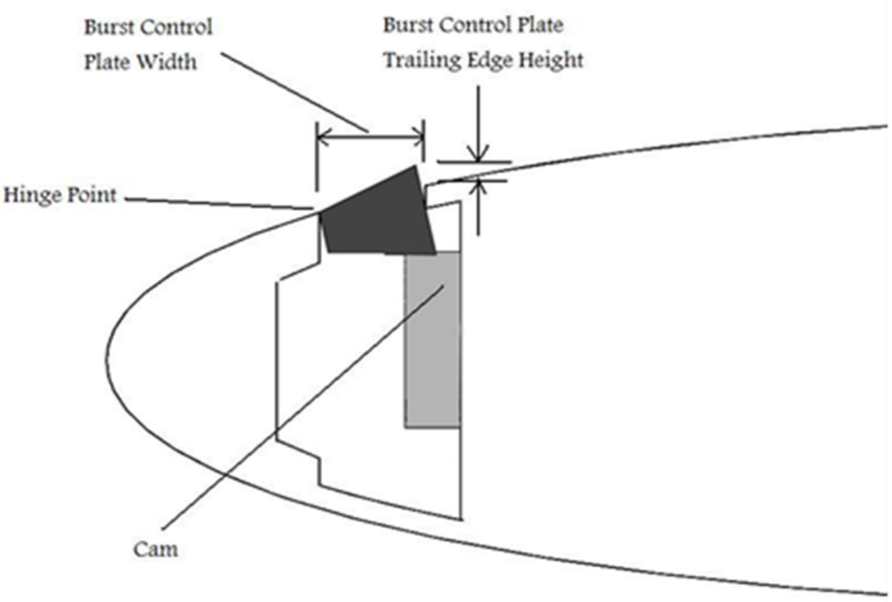

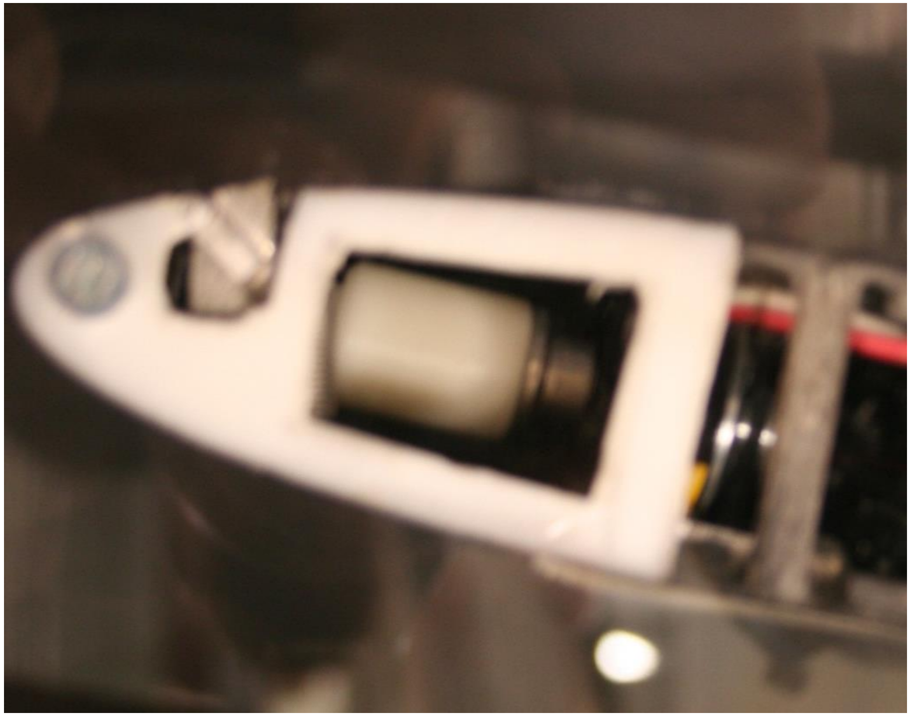

R/C Electric Motor & Cam Shaft

Plate Sizing and Location

- Hinge Point: 5% chord
- Width: 2.5% chord
- Height: 0.5% chord

Conditions

- **Smooth**
- **Stationary (Fully Deployed)**
- **Dynamic (30, 60, 120 Hz)**

Experimental Setup for the Wind Tunnel Testing

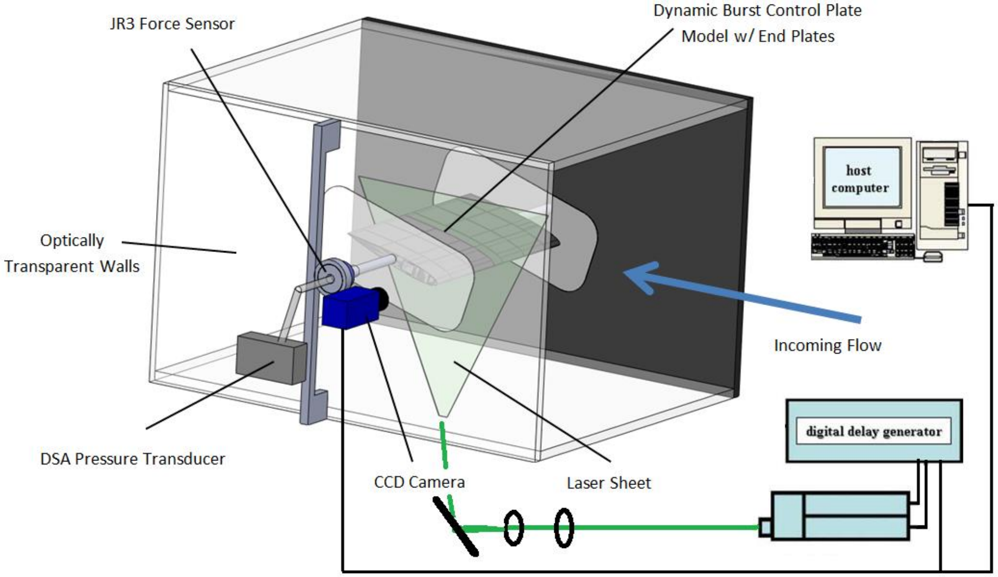

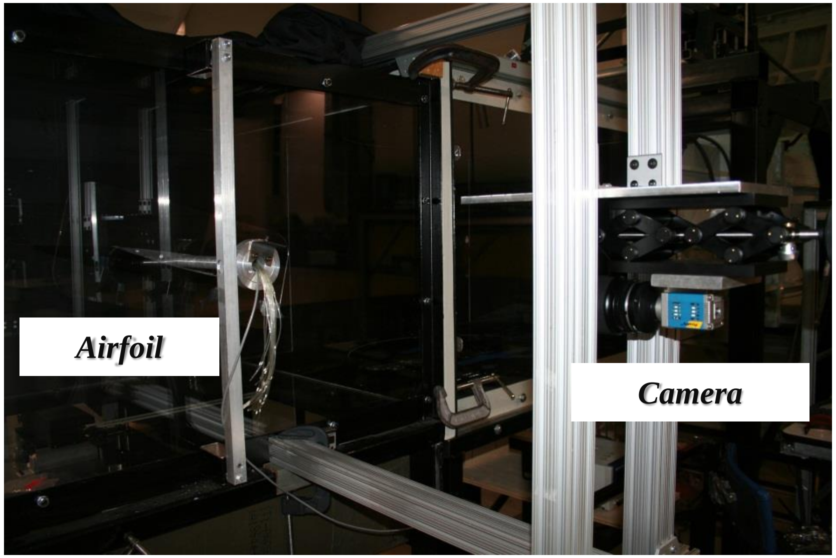

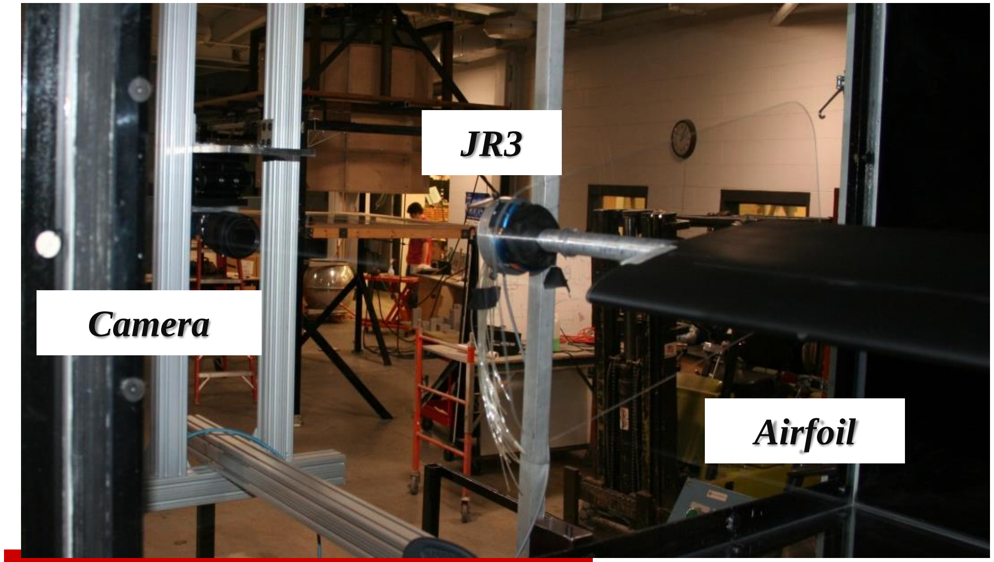

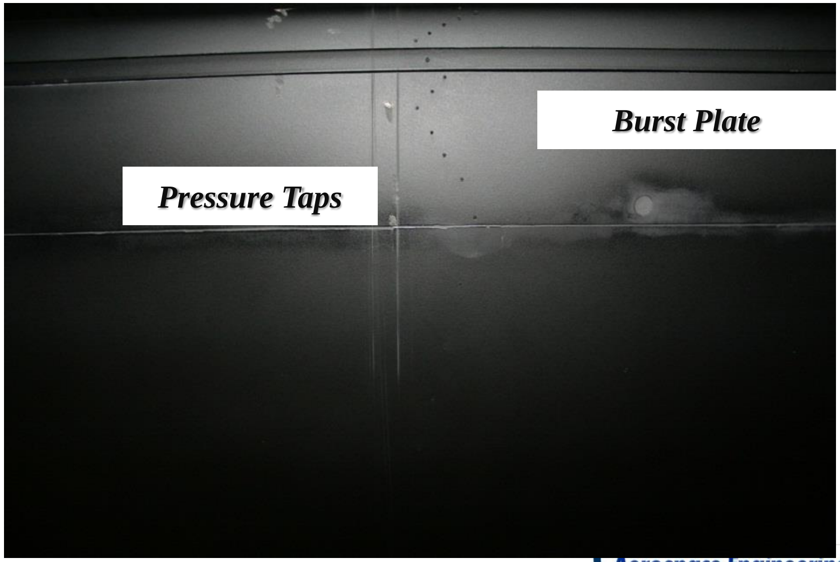

Lift Curve : Force Measurement Data

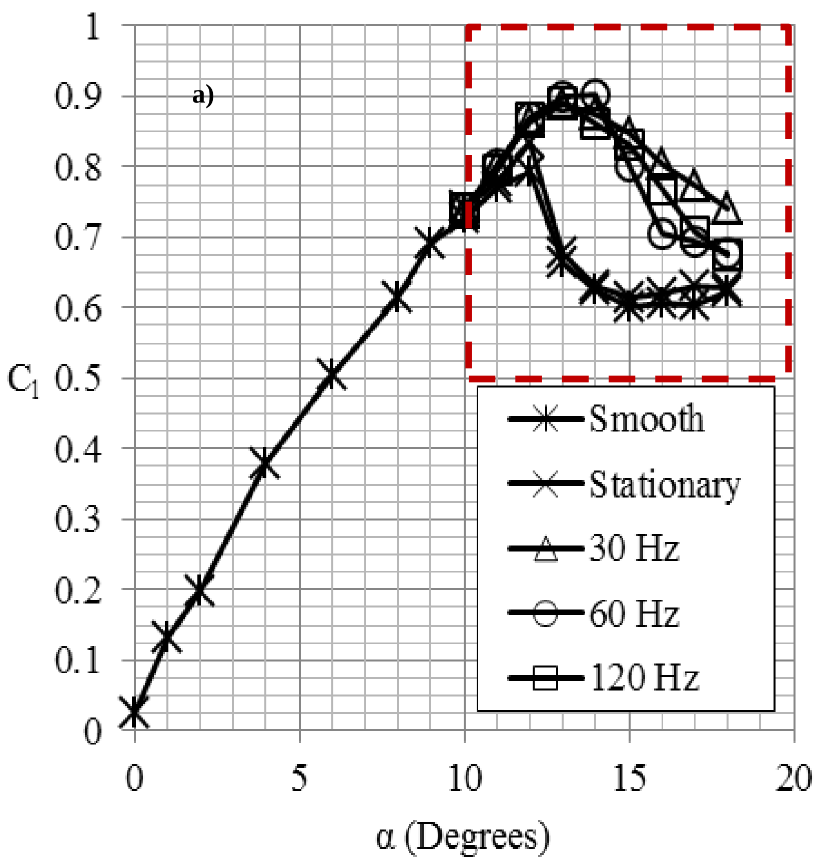

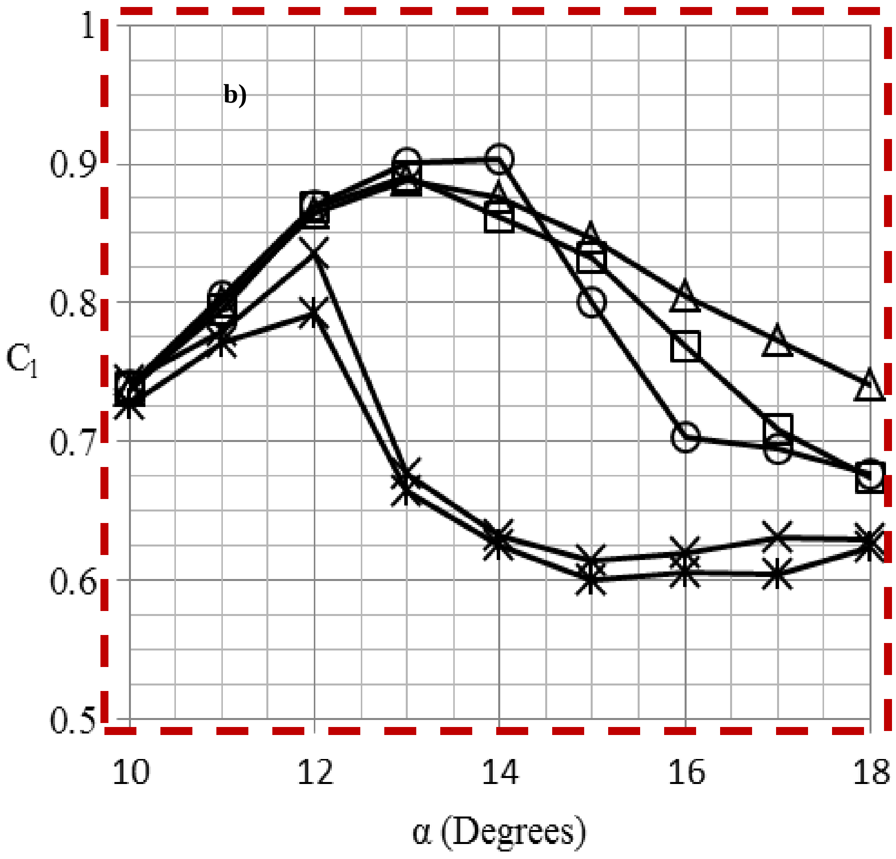

$Re_c = 130,000$

Measured Pressure Distributions

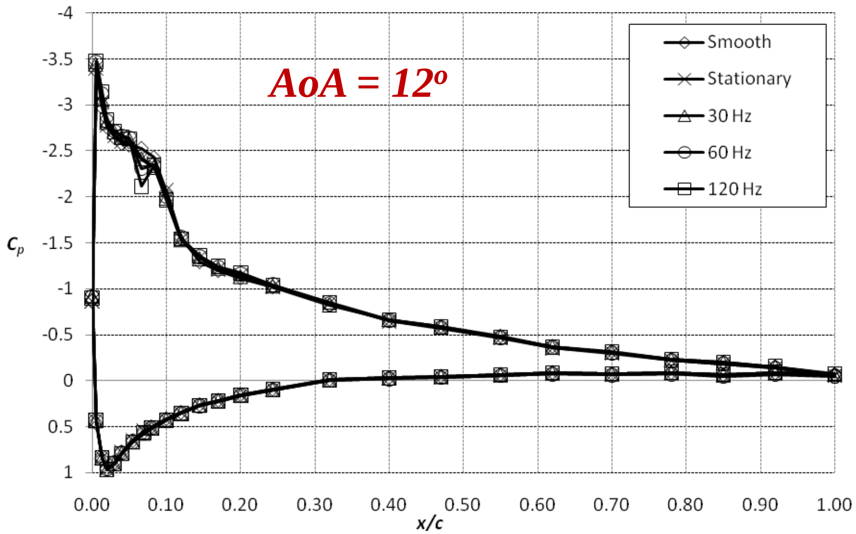

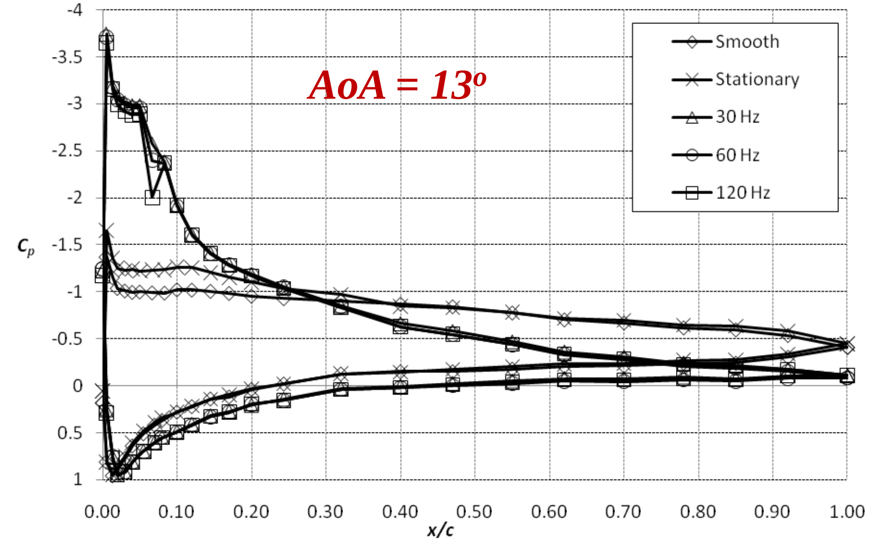

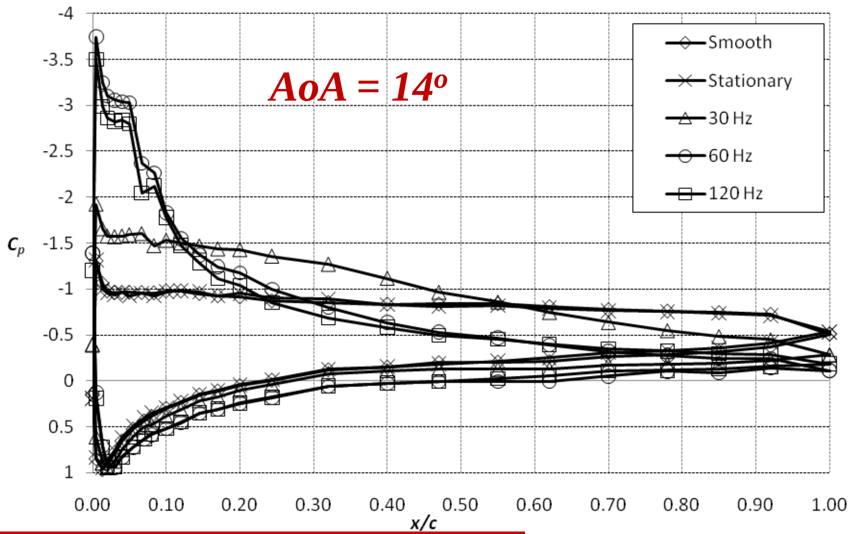

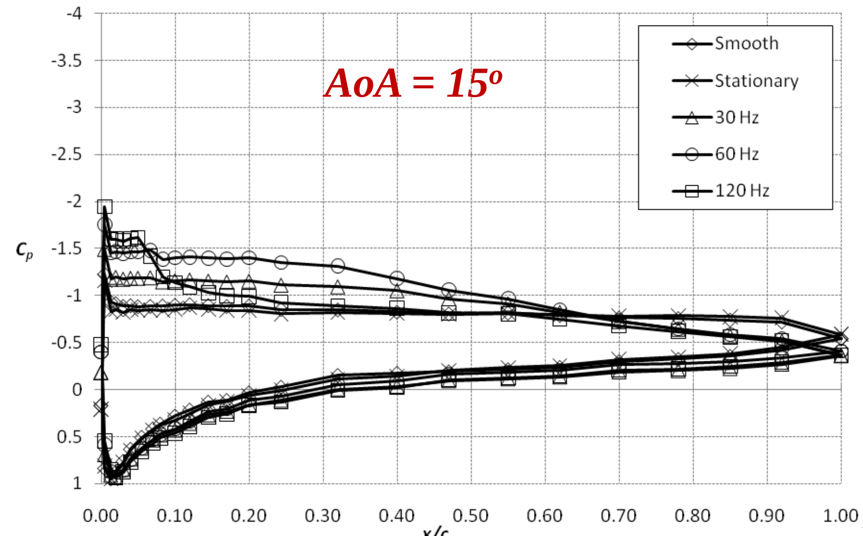

PIV measurements at AOA=14 deg.

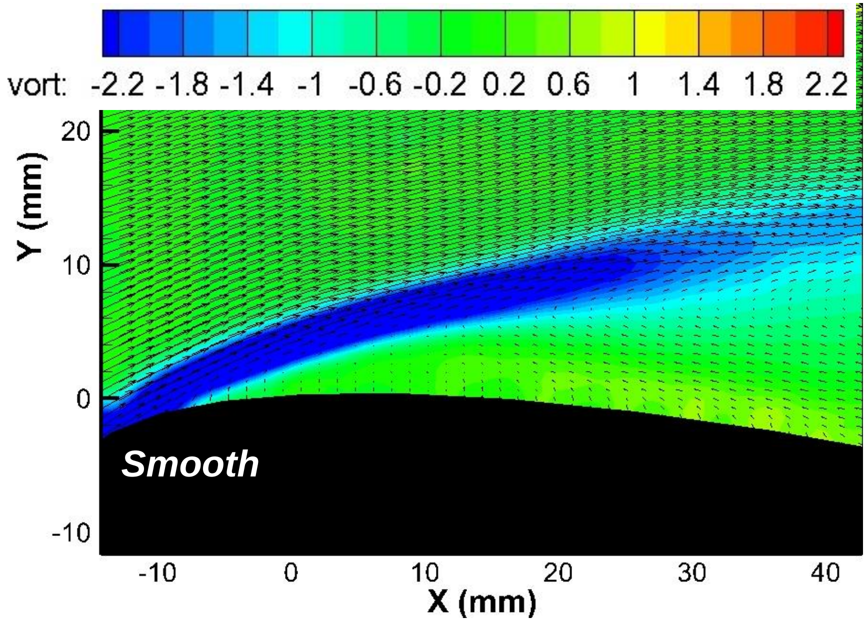

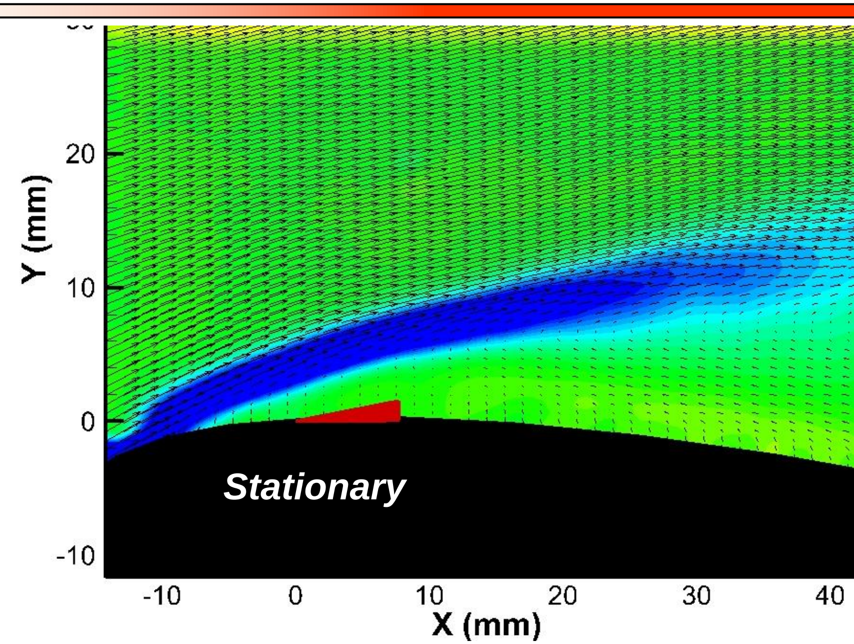

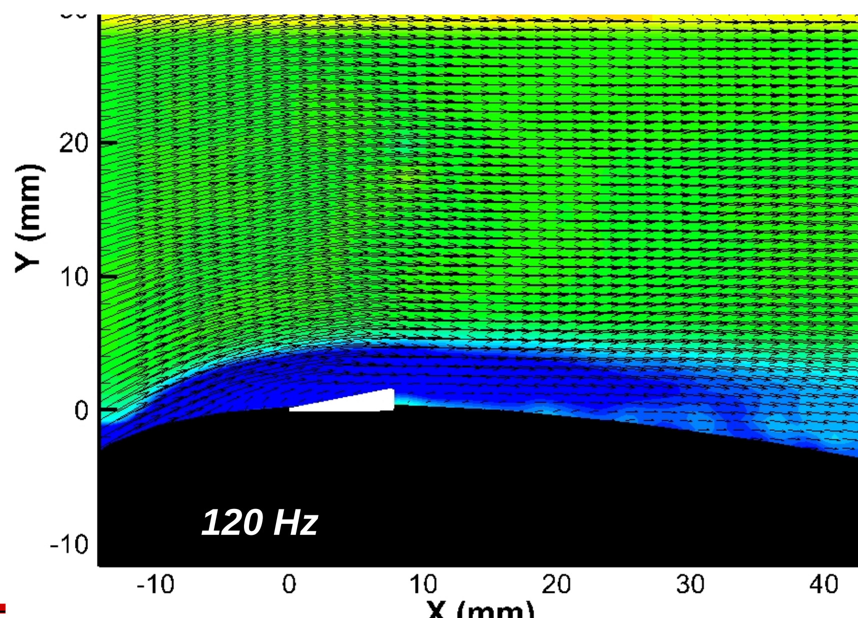

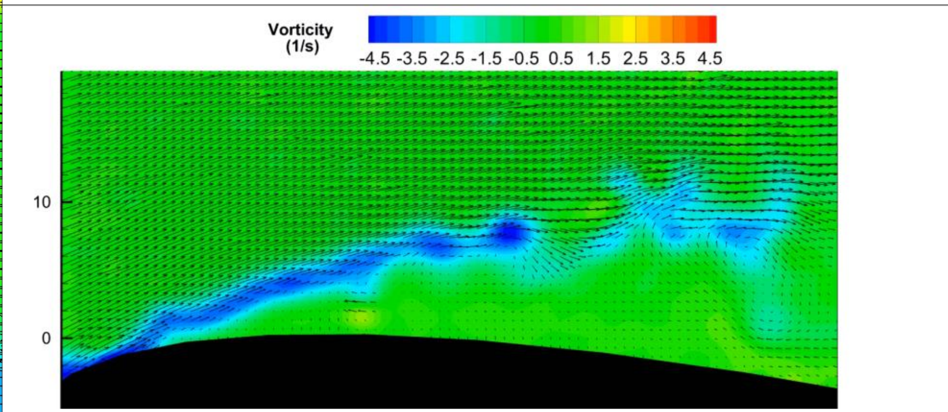

Re_c = 130,000

Phase Averaged Measurement Results

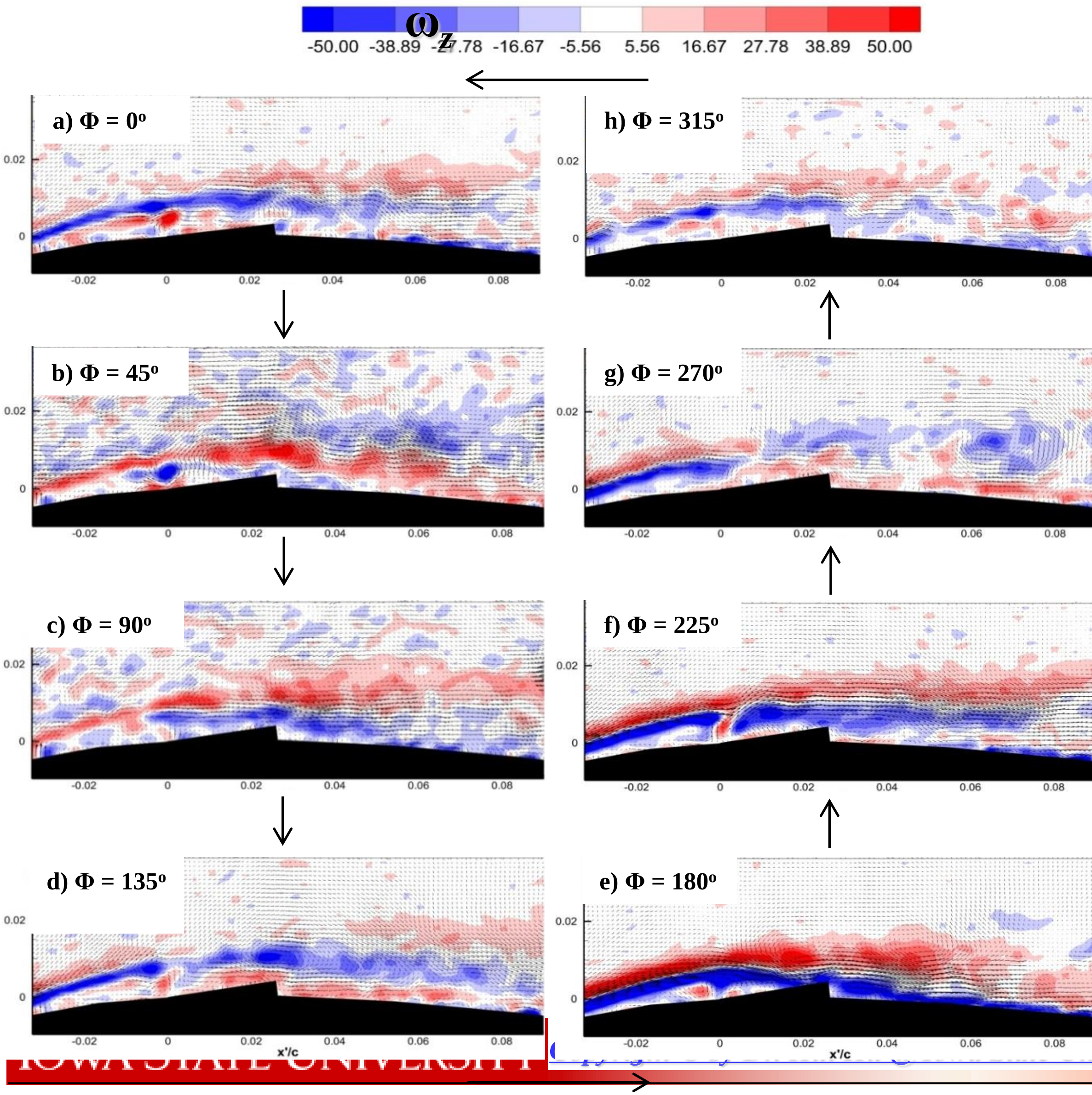

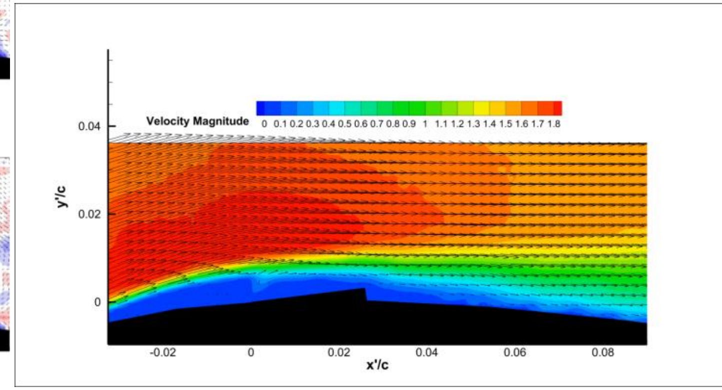

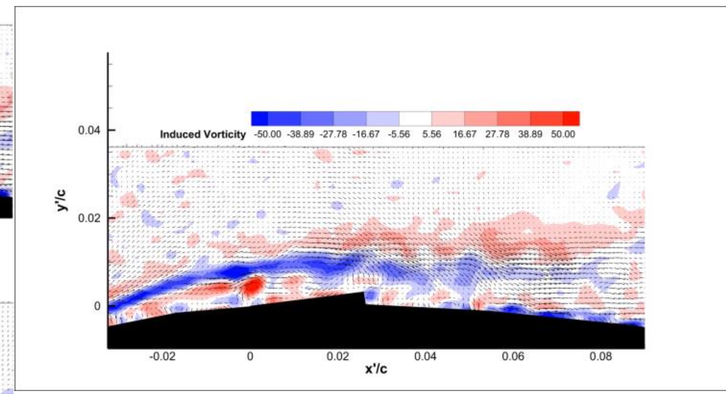

Boundary Layer Flow Separation Control by Using Dynamic Roughness

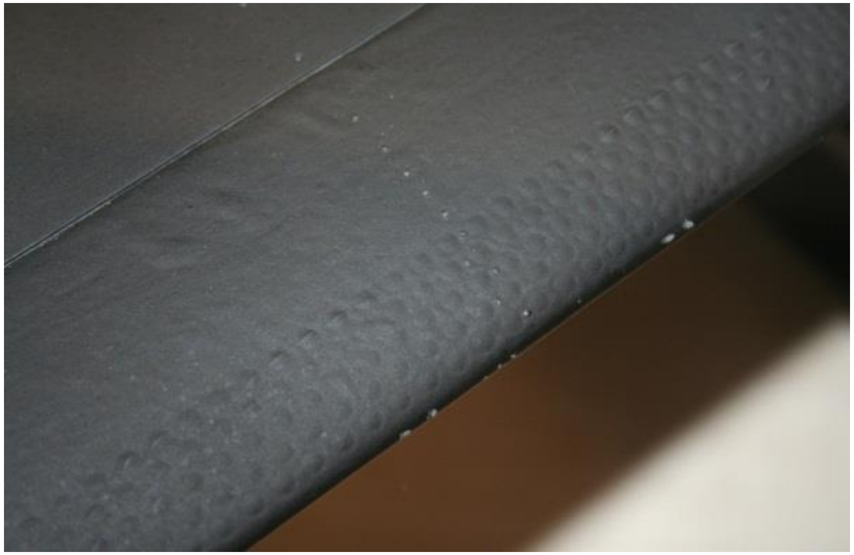

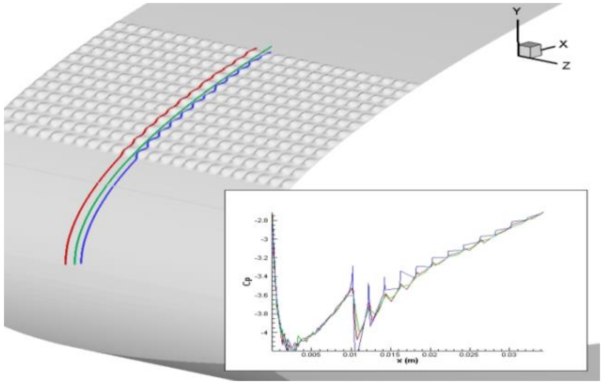

Time Average of 3D Unsteady CFD Using Fluent

Source: Gall, Huebsch & Rothmayer, 2010.

Dynamic Roughness for Boundary Layer Flow Control

- Early 2D CFD results show separation control of LES

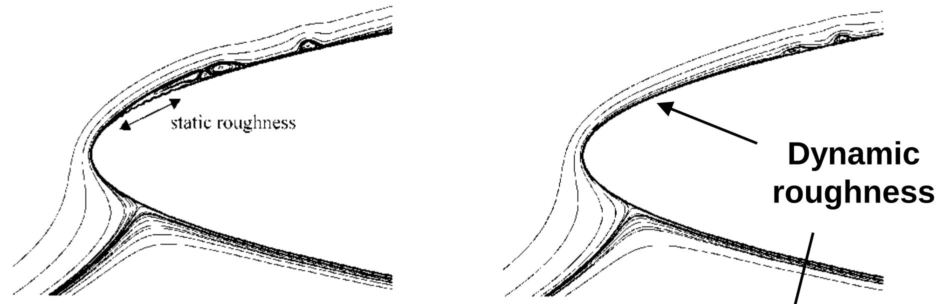

Source: Huebsch, 2004.

- 2D Results confirmed using 3D CFD calculations

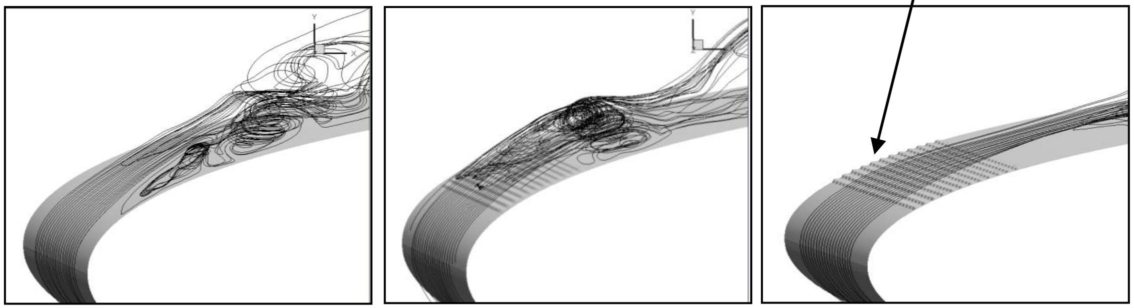

Source: Gall, Huebsch & Rothmayer, 2010.

- Pressurized latex skin over a perforated surface is tested using smoke visualization

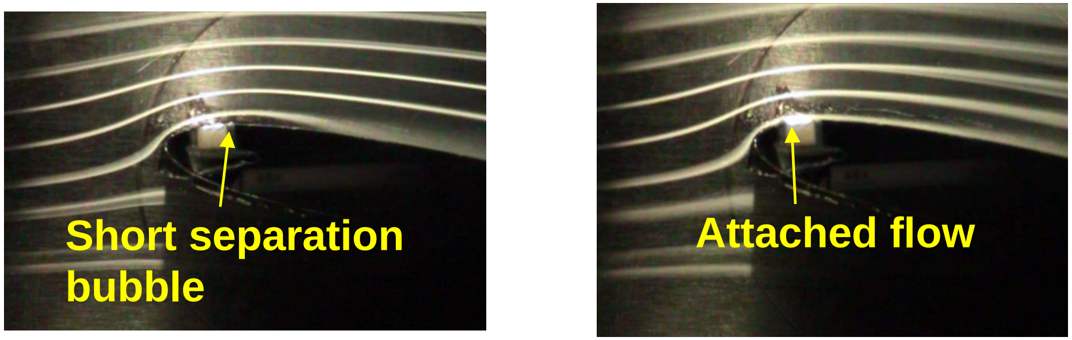

Source: Gall, Huebsch & Rothmayer, 2010.

Local and Global Low-Order Modeling (and CFD, not shown)

Multiple-Scales Boundary Layer Model

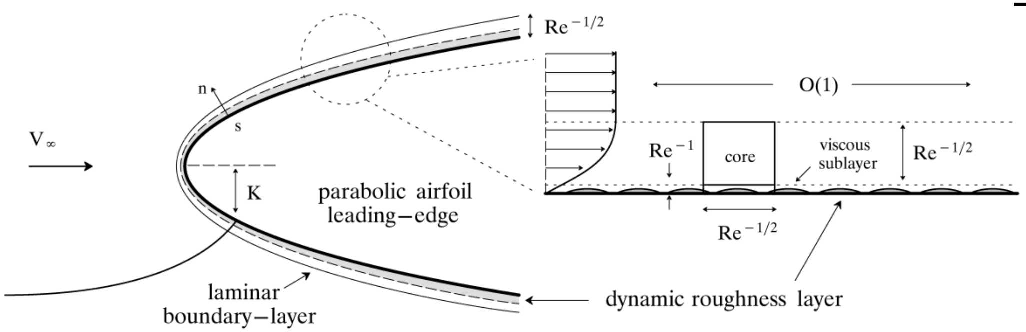

Artificial Reynolds stresses

$$\partial_{T_1}\overline{U}_0 + \partial_{X_1}\left(\overline{U}_0^2\right) + \partial_{X_1}\left[\left\langle\left(\tilde{U}_0 - \left\langle\tilde{U}_0\right\rangle_{T_0}\right)^2\right\rangle\right] + \partial_Y\left(\overline{V}_1\overline{U}_0\right) + \partial_Y\left\langle\left(\tilde{V}_0 - \left\langle\tilde{V}_0\right\rangle_{T_0}\right)\left(\tilde{U}_1 - \left\langle\tilde{U}_1\right\rangle_{T_0}\right)\right\rangle$$
$$+\partial_Y\left\langle\left(\tilde{V}_1 - \left\langle\tilde{V}_1\right\rangle_{T_0}\right)\left(\tilde{U}_0 - \left\langle\tilde{U}_0\right\rangle_{T_0}\right)\right\rangle = -\partial_{X_1}\overline{P}_1 + \partial_Y{}^2\overline{U}_0.$$

Mean flow

Leading Edge Acceleration

$$c_f = \frac{U_e^2}{\sqrt{2\xi}}\frac{\partial F}{\partial \eta}(\xi, 0)$$

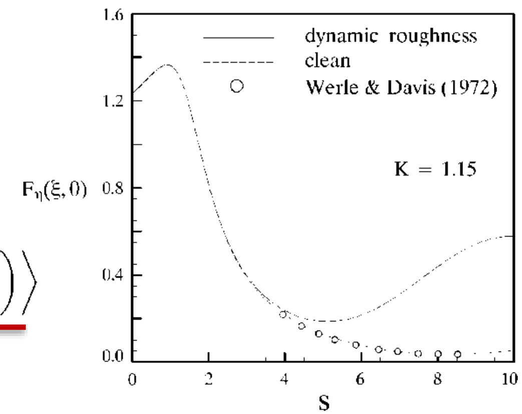

Source: Rothmayer & Huebsch, 2011

Predicted Mean Pressure Drop

$$c_p = (P^* - P_\infty)/\rho_\infty V_\infty^2 = P_e - H^2\omega^2/4$$

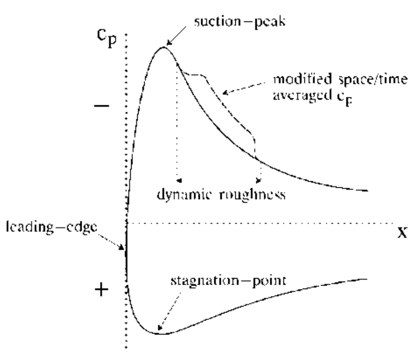

Pressure Drop Confirmed in 3D CFD Calculations

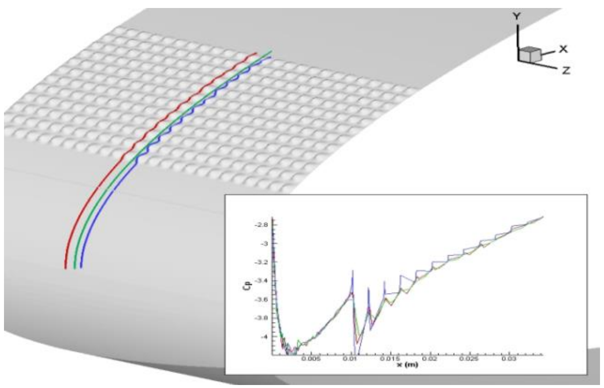

Time Average of 3D Unsteady CFD Using Fluent

Source: Gall, Huebsch & Rothmayer, 2010.

Test Model and Experimental Setup

SolidWorks Design

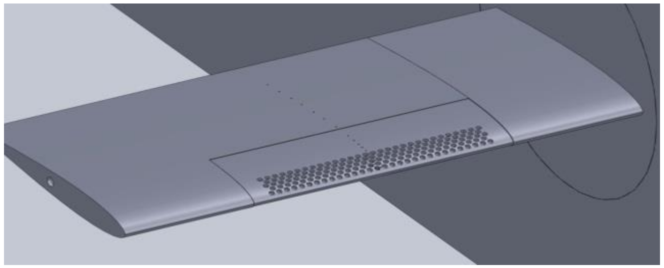

Statically Pressurized L.E.

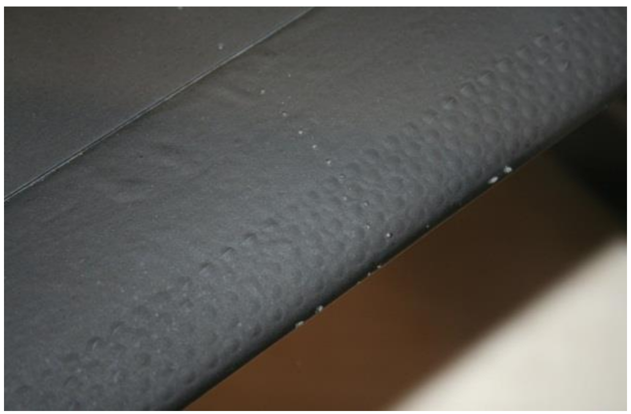

Still from Video of Deformation

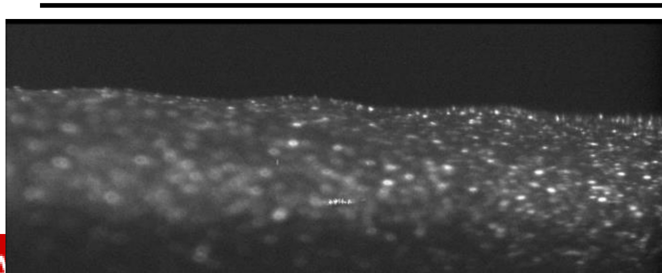

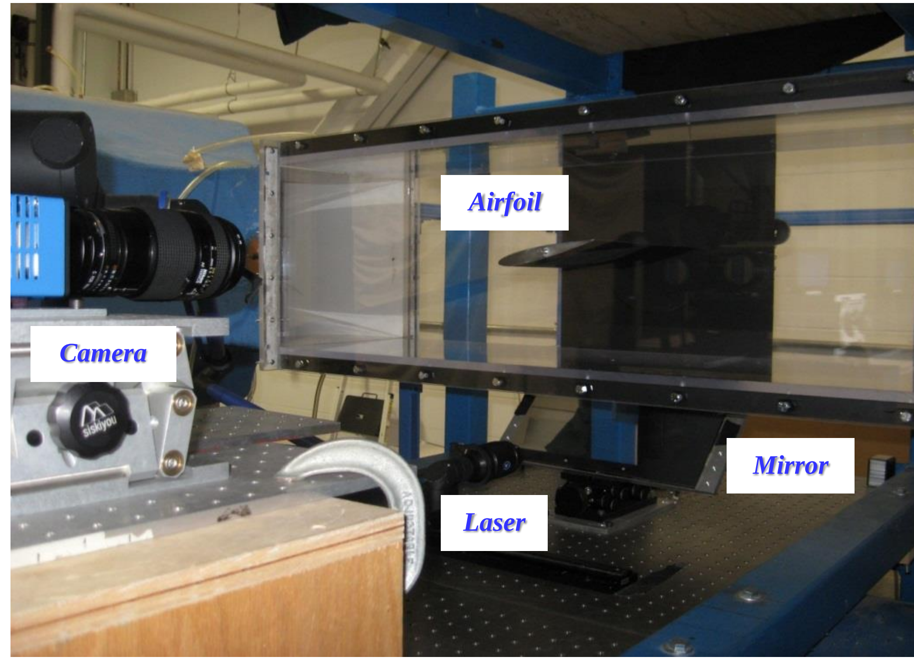

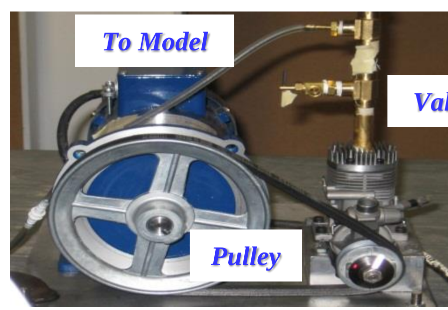

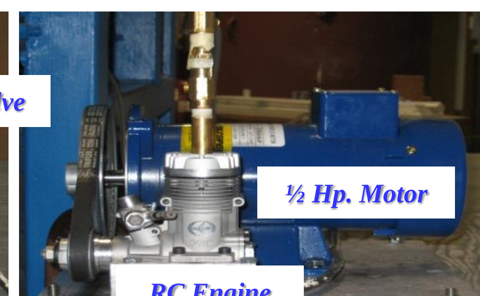

Active Flow Separation Control by Using Dynamic Roughness

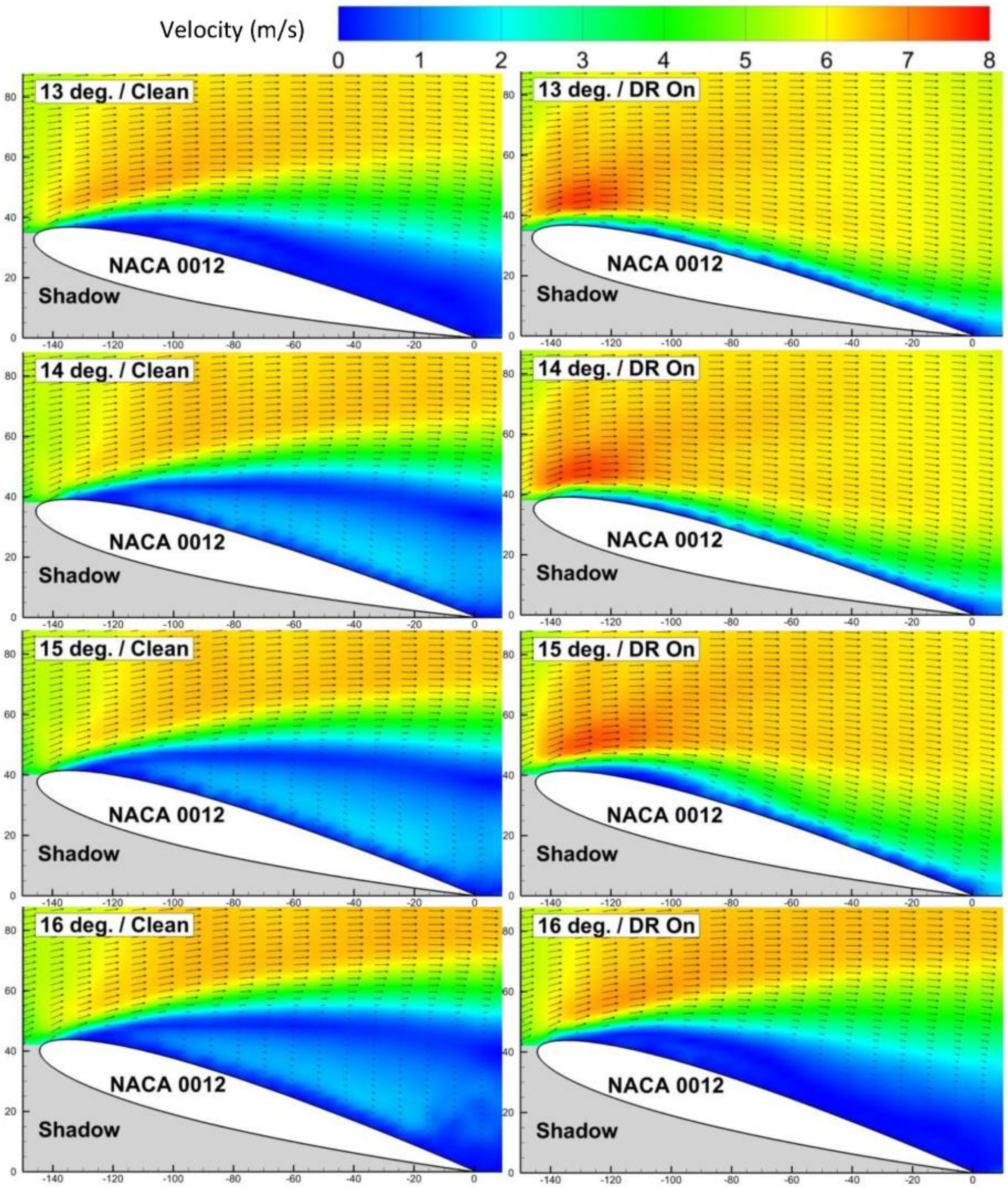

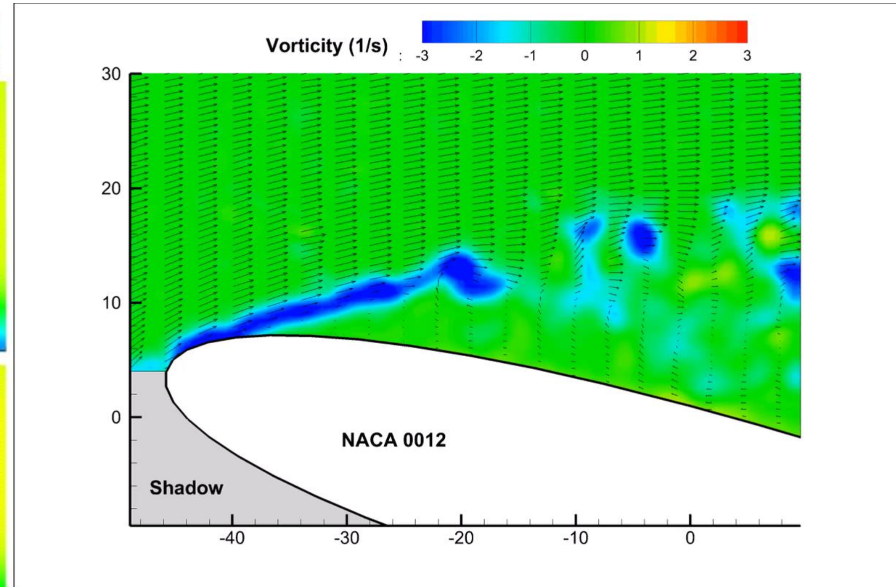

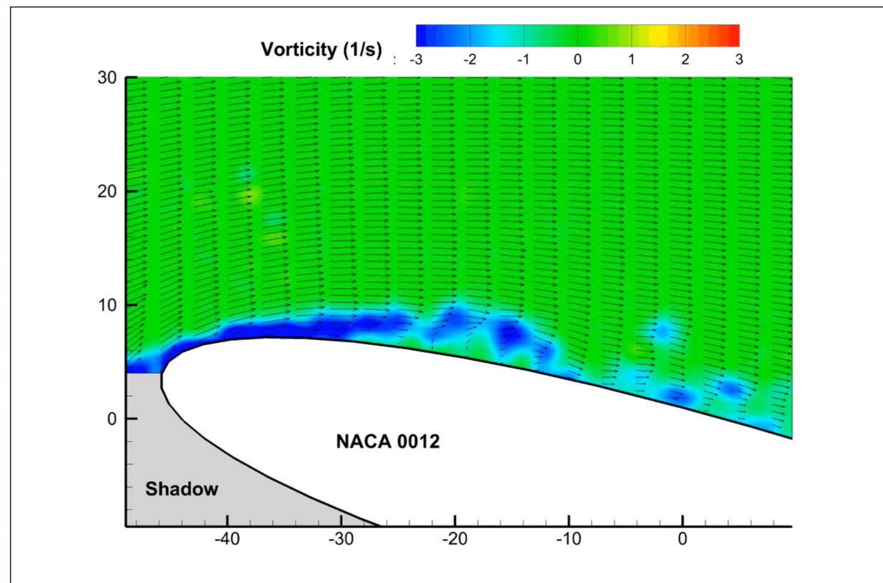

Effects of Oscillation Frequency on Flow Control

Early Prediction of Low Amp. Control

$$c_p = (P^* - P_\infty)/\rho_\infty V_\infty^2 = P_e - H^2\omega^2/4$$

Source: Rothmayer & Huebsch, 2011

3D CFD Prediction of Freq. Toggle

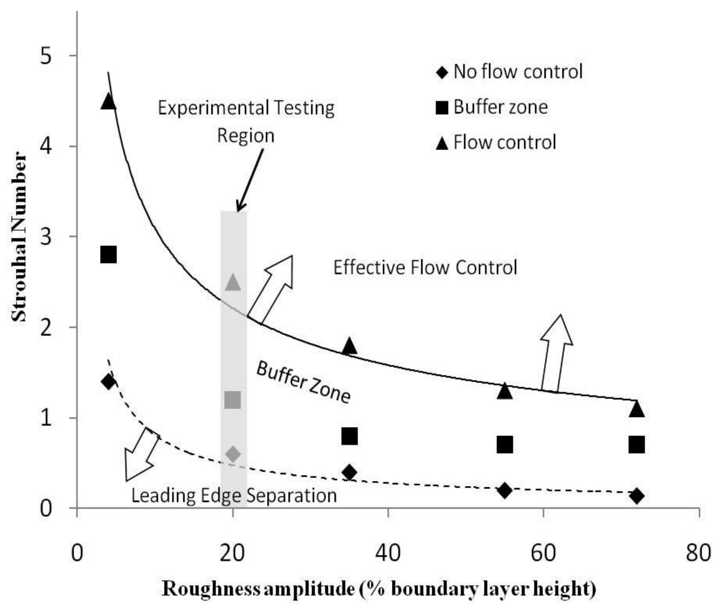

Source: Gall, Huebsch & Rothmayer, 2010 and 2011 (to appear) .

Freq. Sweep at 14 deg Design Case

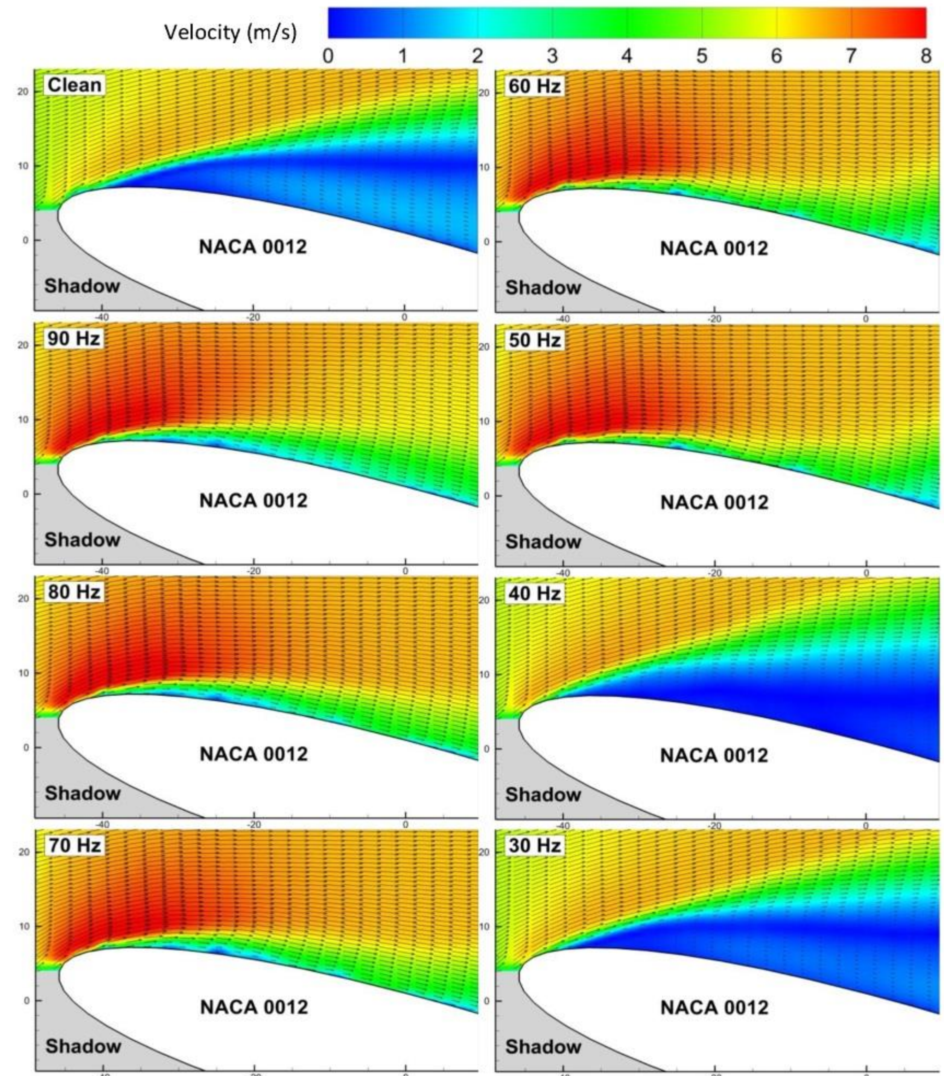

Grager, Hu, Rothmayer & Huebsch (to appear)

Effects of Oscillation Amplitude on Flow Control

Early Prediction of Low Amp. Control

$$c_p = (P^* - P_\infty)/\rho_\infty V_\infty^2 = P_e - H^2\omega^2/4$$

Source: Rothmayer & Huebsch, 2011

3D CFD Prediction of Freq. Toggle

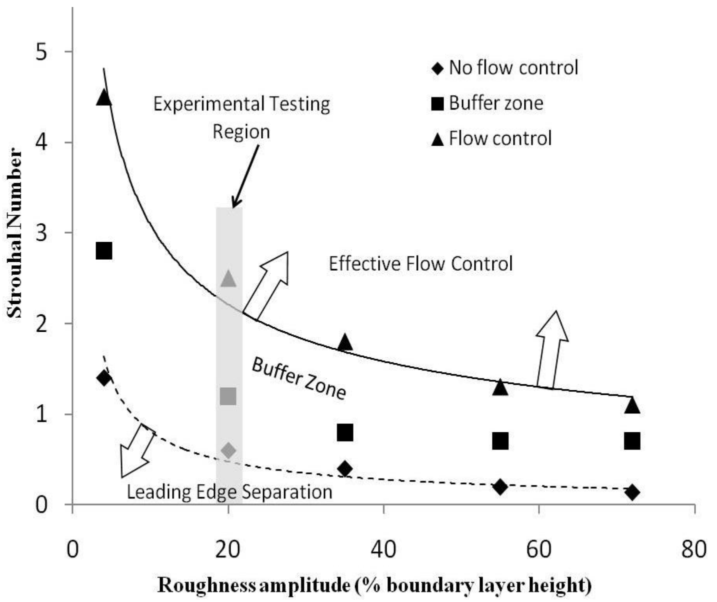

Source: Gall, Huebsch & Rothmayer, 2010 and 2011 (to appear) .

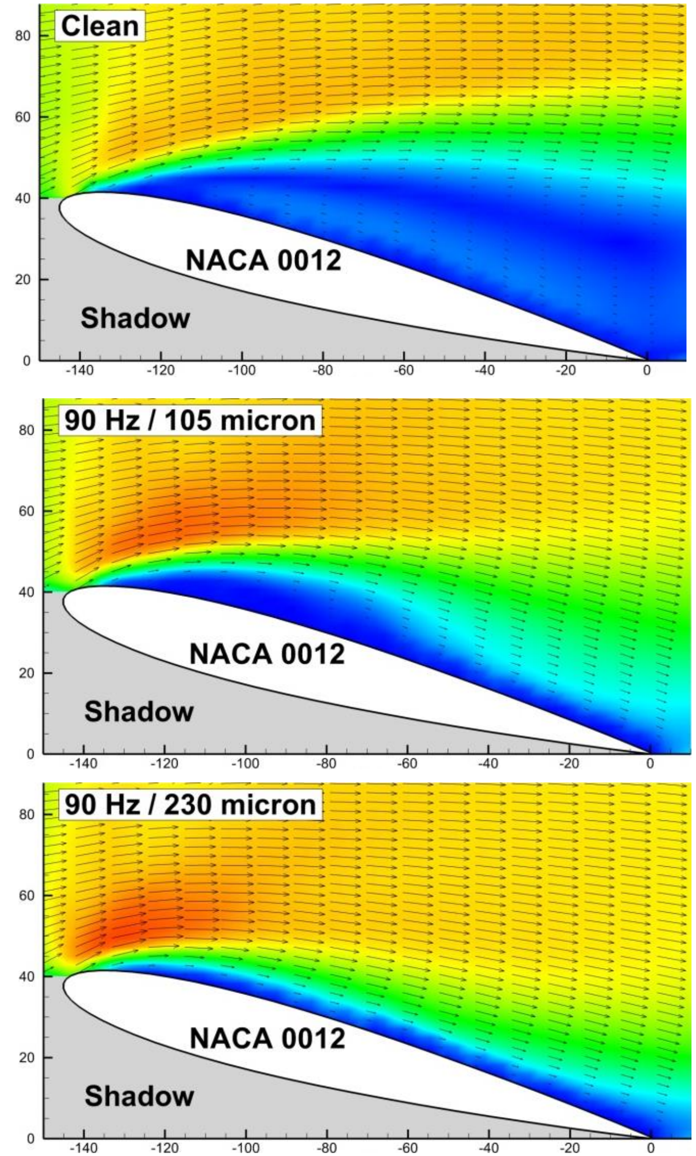

Test conditions: Re=75K, AOA=15 Deg.

Grager, Hu, Rothmayer & Huebsch (to appear)

Morphing Airfoil Designs

https://www.youtube.com/watch?v=L5KKumkXTqo

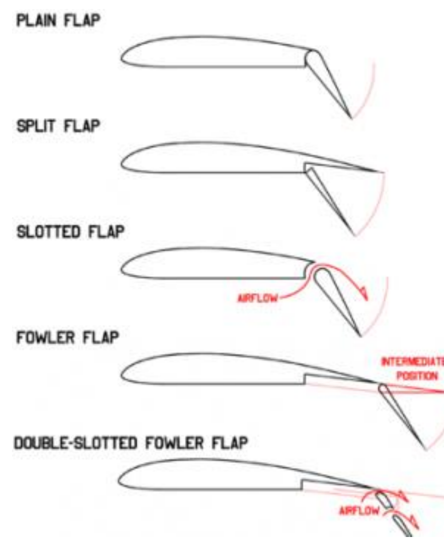

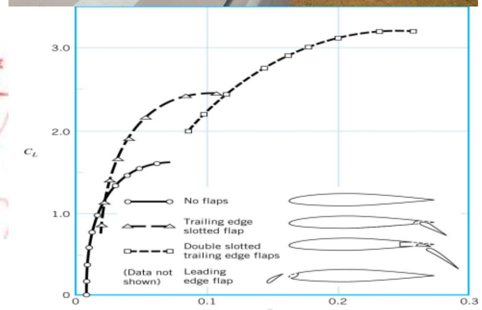

- https://www.youtube.com/watch?v=9ZpAHxMj5IU